[Catégorie ]

# SPICE WP5: Radar wave interaction with the snowpack

| | |
|---|---|
| Reference: | CLS-SPA-18-023 |
| Nomenclature: | - |
| Issue: | 1. 2 |
| Date: | 2018,Jul.04 |

**CLS** headquarters
11 rue Hermès
Parc technologique du Canal
31520 Ramonville Saint-Agne
FRANCE

Tel. +33 (0)5 61 39 47 00
Fax +33 (0)5 61 75 10 14
Mail: info@cls.fr
www.cls.fr

CLS Brest Le Ponant
Zone du technopôle de Brest Iroise
Avenue La Pérouse
29280 Plouzané
FRANCE

Tel. 33 (0)2.98.05.76.80
Fax 33 (0)2.98.05.76.90

## Chronology Issues:

| Issue: | Date: | Reason for change: | Author |
|---|---|---|---|
| 1.0 | 26/02/2018 | Creation | J.Aublanc |
| 1.1 | 04/07/2018 | Modified document after ESA review | J.Aublanc |
| 1.2 | 24/07/2018 | Modified document after ESA review | J.Aublanc |
| | | | |
| | | | |
| | | | |

## People involved in this issue:

| | | |
|---|---|---|
| Written by (*): | J.Aublanc<br>F.Remy | Date + Initials:( visa or ref)<br>10/04/2018 |
| Checked by (*): | | Date + Initial:( visa ou ref)<br>[Checker] |
| Approved by (*): | P.Thibaut | Date + Initial:( visa ou ref)<br>[Approver] |
| Application authorized by (*): | | Date + Initial:( visa ou ref) |
| Accepted by ESA | Jérôme Benveniste | Date + Initial:( visa ou ref) |

*In the opposite box: Last and First name of the person + company if different from CLS

## Index Sheet:

| | |
|---|---|
| Context: | |
| Keywords: | SPICE, Cryosat-2, AltiKa, Antarctica, altimetry, LRM, SAR |
| Hyperlink: | |

## Distribution:

| Company | Means of distribution | Names |
|---|---|---|
| | | |

FORM-NT-GB-10-1

# List of tables and figures

## List of tables:



## List of figures:

# Reference documents

**RD-1 SPICE Product Validation Report**

**RD-2 SPICE Retrackers' Performance Technical Note v1.1**

**RD-3 SPICE ATBD v2.1**

## List of Contents

# 1. Introduction

The Sentinel-3A spacecraft was launched on February 16 2016, and is the first mission to fully operate in SAR altimetry mode. The mission is primarily dedicated to oceans, but allows monitoring the polar regions with its high inclination orbit (81.35°). Thanks to the along-track resolution of 300 meters reached in Synthetic Aperture Radar (SAR) mode, it has the potential to provide repeated and accurate measurements over the polar ice sheets.

The ESA SPICE project (Sentinel-3 Performance Improvement for Ice Sheets), has worked in advance of the operational phase of Sentinel-3 to assess and improve SAR altimetry over the polar ice sheets. The study is performed thanks to a specific set of SAR mode Cryosat-2/SIRAL data, acquired in a limited space and time period over the Antarctic ice sheet.

A first project work package purpose is to develop L1 and L2 processing dedicated to SAR altimetry. A second work package goal is to compare SAR and P-LRM performances over the polar ice sheets. Finally, a third work package is dedicated to the study of the radar wave interaction with the snowpack. SPICE project includes two phases: a first phase during which existing and conventional L1/L2 SAR altimetry processing are developed and evaluated. Based on the results earned at the end of phase 1, a second phase aims at improving the L1/L2 processing to get the best performances possible in term of measure precision and accuracy.

This document presents the results obtained for the work package dedicated to the radar wave interaction with the snowpack. A cross-comparison between Cryosat-2 and AltiKa is performed and shows Ku and Ka bands sensitivity to volume scattering effect. This sensitivity is assessed on the shape of the waveform measured and on the surface elevation estimated by retracking.

## 2. Scientific background

The main challenges for radar altimetry over ice sheet surfaces relate to the ground footprint size and the complex nature of the snow/ice medium with which the radar signal interacts. As the Ku band signal penetrates into the snowpack, measure is sensitive, not only to surface properties, but also to the snowpack properties. The backscattered energy comes from the surface but also from subsurface: this is commonly called the volume scattering effect. Altimeter waveform measured over ice sheets can be expressed as the sum of a surface waveform and a subsurface waveform:

- The surface waveform is sensitive to a complex surface roughness, variable topographic slopes (up to several percent), small/medium scale topographic structures (sastrugi, mega-dunes), rugged terrain…

- The subsurface signal has two origins: the reflections of the snowpack internal layers [Rott et al. 1993] and the snow grain scattering [Ridley & Partington, 1988]. Altimeter signal is also attenuated by absorption loss within the snowpack. The subsurface waveform is sensitive to snowpack properties, variable in time and space. Scientific surveys demonstrate that these properties are mainly: snowpack stratification, snowpack temperature, snow grain size and snow density [Remy and Parouty, 2009].

The comparison of measurements in Ku and Ka frequencies allows us to understand and better quantify the penetration properties of the radar waves and their consequences on the altimetry measure. Over water surfaces, Ku and Ka signals reflect at the air/water interface. Over snow or ice, it is commonly understood [Vincent et al., 2006] that the radar wave penetrates the ice pack if its wavelength is larger than the snow grain size (typically 0.5 mm but grain size depends on the temperature (snow metamorphism) and snow accumulation).

Ku and Ka band signal wavelengths are respectively 2.21cm and 0.84cm. The factors between signal wavelength and grain size (0.5mm) are respectively 44 and 17 in Ku and Ka bands. Empirical analyses [Legresy & Remy, 1998] show that Ku-band radar penetration above the dry snowpack of Antarctica is between 5 meters in the interior to 14 meters at a lower altitude. In Ka-band, following Mie theory, the scattering coefficient is inversely proportional to the radar wavelength at a power of 4. From Ku to Ka bands, the scattering coefficient will consequently increase by a factor 55. This leads to a penetration depth over the snow surface between 0.1 meter and 0.3 meter in Ka band [Vincent et al., 2006].

First analyses of the surface elevation estimated by AltiKa confirmed the previous assumptions about the weak sensitivity of the Ka band to volume scattering. A study from Michel et al. [2014] estimated the penetration depth of Ka-band at 0.3 meter.

# 3. Dataset

## 3.1. Cryosat-2

### 3.1.1. SAR mode acquisitions over Antarctica

Through its high inclination orbit, the Cryosat-2 mission goes up to 88° N/S in latitude, surveying most of the entire Antarctic continent. In the normal course, Cryosat-2 operates in the altimeter Low Resolution Mode (LRM), over a large part of the Antarctica ice sheet (notably in the interior of the continent), as requested by the land ice user community. It also operates in an innovative SAR Interferometric (SARIn) mode over the Antarctica margins where surface is steep and rugged and therefore badly monitored by conventional altimeters.

Cryosat-2 has been sporadically operated in SAR altimetry mode over Antarctica to help characterize the Sentinel-3A ground processing algorithms over typical rough ice-covered topography terrain. This experimental acquisition was carried out over three small zones (Lake Vostok, Dome-C and the Spirit zone) for a limited period of time in winter 2014. The figure below shows the location of these three sites with SAR Cryosat-2 tracks superimposed:

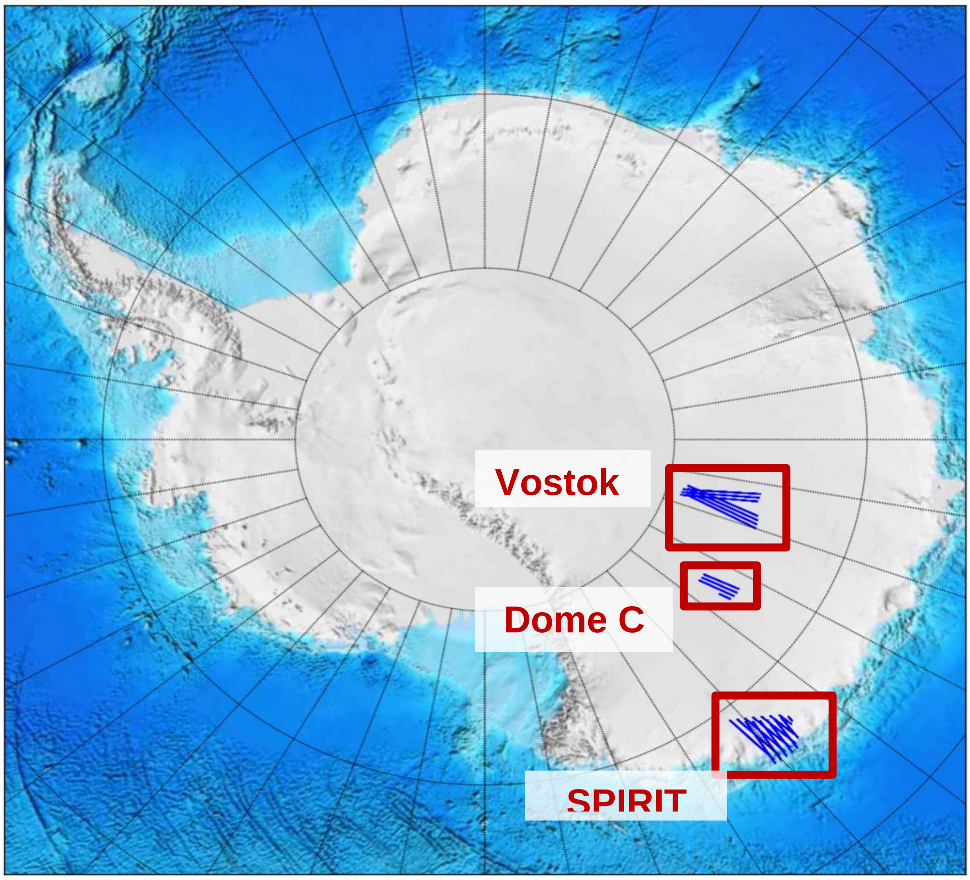


*Figure 1: Location of the three sites (red boxes) where Cryosat-2 has been operated in SAR mode over Antarctica in winter 2014. Cryosat-2 tracks are displayed in blue color.*

### 3.1.2. Cryosat-2 SAR altimetry

***General statements***

The SIRAL altimeter on board the ESA Cryosat-2 satellite has been the first radar instrument able to operate in high-resolution mode (SAR) before the Sentinel-3 series. SAR altimetry processing involves **a delay/Doppler technique** applied on a burst of correlated pulses. By exploiting the frequency variations caused by the Doppler effect to the backscattered signals on-ground, this technique samples and separates the ground surface on contiguous Doppler bands arranged across the track. This results in a much finer along-track spatial resolution of the Earth's surface than conventional pulse-limited altimeters.

When operating in SAR mode, Cryosat-2 sends bursts of 64 pulses at a Pulse Rate Frequency (PRF) of 18kHz around (PRF of pulses inside the burst). With such a configuration the width of the Doppler bands, i.e. the along-track resolution, obtained is around **300m**. The gathering of multiple contributions, to a same Doppler strip on-ground reduces significantly the speckle noise. This is commonly called the SAR multi-looking processing, as performed in the ESA Payload Data Ground Segment (PDGS) or in the CNES Cryosat-2 Processing Prototype (CPP) [Boy et al., 2017]. Information's regarding the PDGS products and the SAR processing can be found online through the ESA website. (http://emits.sso.esa.int/emits-doc/ESRIN/7158/CryoSat-PHB-17apr2012.pdf). More detailed information about the SAR altimetry concept and processing can also be found in Raney [1998].

In parallel to the SAR processing, it is also possible to exploit radar pulses in a conventional way. The averaging of 256 pulses of 4 successive bursts per cycle generates Pseudo-LRM measurements. Considering that only one in eight returned pulses per burst are effectively de-correlated, the measure noise is degraded compared to conventional LRM, explaining the "Pseudo" terminology used.

***SAR and P-LRM footprints***

By reducing the along-track footprint on-ground, the SAR measure brings theoretically two major advantages over ice sheet surfaces compared to conventional altimetry:

1) An ability to retrieve finer topographic scales: The pulse limited footprint is defined as the illuminated area on ground around at the nearest point of the surface (generally referenced as the Point Of Closest Approah (POCA)). The POCA is estimated by retracking in the waveform leading edge part. Considering a leading edge width of 4 range gates, the Cryosat-2 pulse limited footprint is 1.66km radius in LRM, covering an area of around 8.65 $km^2$. In SAR mode the footprint is reduced to a strip of around 3.32km long and 300 meters large, covering an area of around 1 $km^2$.

2) A weak sensitivity to the slope-induced error in the along-track direction: In practice, the range estimated in conventional altimetry generally corresponds to the distance between the antenna and the POCA [Brooks et al., 1978]. Over a flat surface, such as the ocean, the POCA is located at nadir. Elsewhere, for a more irregular topography, the POCA is shifted in the upslope direction of the surface.

As a direct consequence of the second point, in case of along-track slope, the POCA does not originate from the same location on-ground for a co-dated SAR and P-LRM measurement. This complicates comparisons at crossovers between SAR mode and P-LRM measures. Note that the across-track slope sensitivity is the same for both SAR mode and P-LRM.

The following figures display the respective SAR mode and P-LRM footprints, in case of flat surface (top) and in case of along-track slope (bottom):

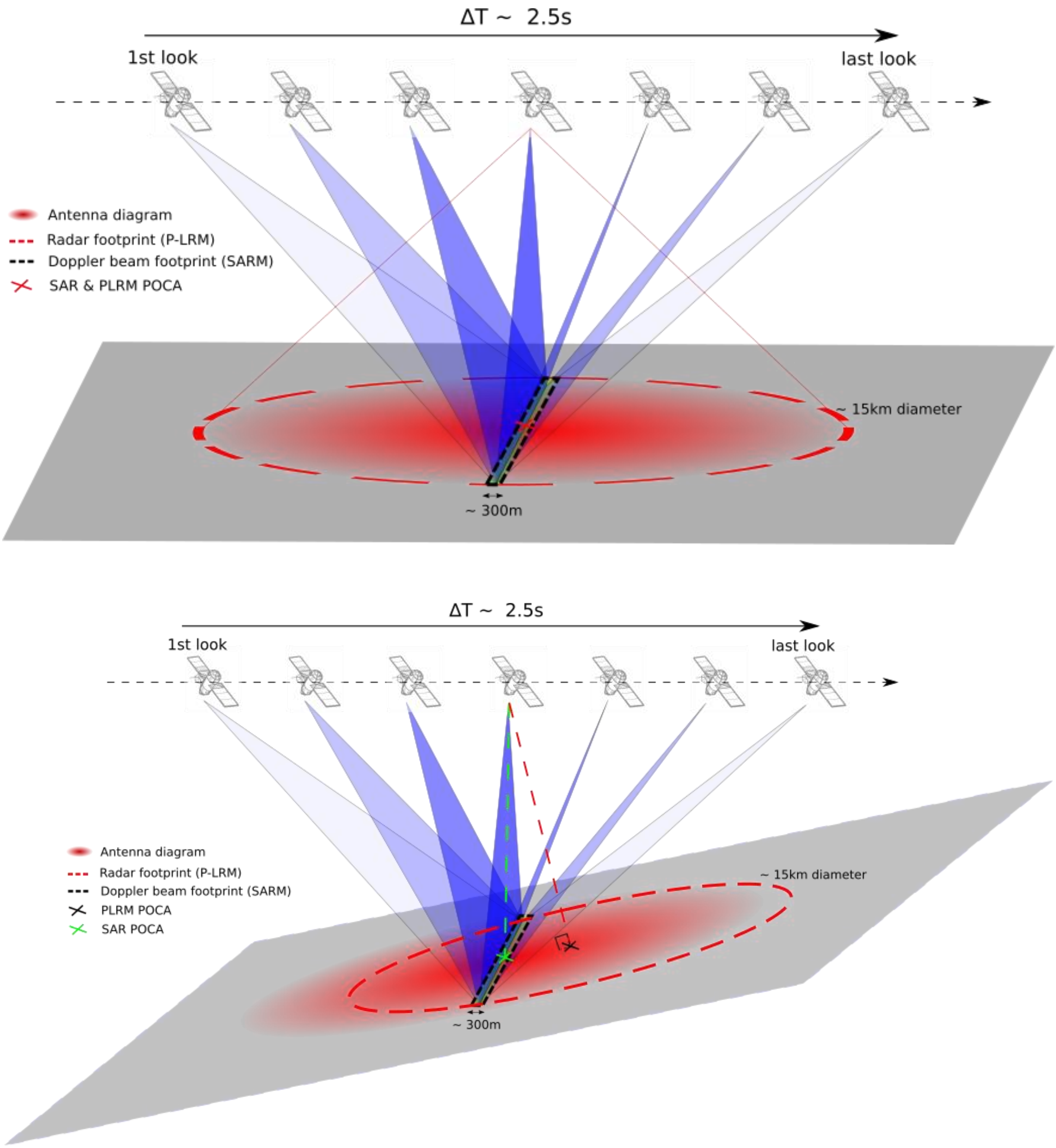


*Figure 2: Diagram of a Cryosat-2 measurement in LRM and SAR modes. In LRM, a wide circular area (of nearly 15 km) on a flat surface is illuminated by the conical beam of one radar pulse (red dotted circle). In SAR mode, multiple synthesized beams formed at several satellite positions, are combined over the same strip to create a multi-looked waveform. This Doppler cell (black dotted strip) is 300 m along the track, and approximately 15 km wide.*

The slope-induced errors on the altimeter range (**Δh**) and the offset on ground between nadir and POCA (**Δx**) can be retrieved using the following equations [Wingham et al., 2004; Sandwell and Smith, 2014]:

$$\Delta x = s * \ He \qquad ; \qquad \Delta h = \frac{s^2 * He}{2} \qquad (1)$$

where ***s*** is the surface slope (%), ***R*** the Earth radius and ***He*** the effective altitude of satellite given by: $\mathrm{He} = \frac{\mathrm{H}}{1+\mathrm{H/R}}$.

As the slope-induced error on the altimeter range depends of the square of the surface slope, errors quickly increased with the surface slope intensity. For example, taking the nominal Cryosat-2 orbit (725 km) the error is 2cm for 0.025% of slope, 2 meters for 0.25% of surface slope and 32 meters for 1% of surface slope (see Figure 10).

### 3.1.3. SPICE level-1 and level-2 processing

The SPICE project is divided in two main phases:

- One first phase during which Cryosat-2 SAR mode and P-LRM acquisitions are processed and evaluated using conventional L1/L2 algorithms.
- One second phase during which innovative L1/L2 processing are implemented and evaluated for both modes (WP3 & WP4 objectives). Finally, based on a validation performed during WP4, the most performant processing baselines are selected to produce phase-2 dataset.

The following table shows L1/L2 processing selected for generating the phase-1 and phase-2 products. Following the Product Validation Report (R-D1), only the most performant algorithms are presented on this table. All these processing are presented in more details in the Product Validation Report (RD-1)

| | | Phase-1 | Phase-2 |
|---|---|---|---|
| **P-LRM** | **level-1** | **/** | **Zero-padding factor 2** |
| | **level-2** | **TCOG (ICE-1) retracker (30%)** | **TCOG (ICE-1) retracker (50%)**<br>**Batch processing** |
| **SARM** | **level-1** | **/** | **Zero padding factor 4** |
| | **level-2** | **TPR retracker (75%)** | **TPR retracker (75%)**<br>**DEM to identify WF peak** |

***Table 1: level-1 and level-2 processing used for generating phase-1 and phase-2 products in P-LRM (top) and SARM (bottom)***

A first series of Ku/Ka comparisons and analyses were performed after phase-1. This helped setting up the Ku/Ka comparison methods and developing dedicated algorithms for this study. Moreover, at the end of phase-1, a validation of the geophysical corrections and the estimated surface elevation was achieved to ensure the data consistency and the correct interpretation of Cryosat-2/AltiKa differences.

=> **This technical note presents results achieved when using the final phase-2 dataset.**

## 3.2. AltiKa

### 3.2.1. Mission characteristics

SARAL (Satellite with ARgos and ALtiKa) is a satellite mission resulting from a french and indian collaboration (CNES and ISRO). It was launched on February 2013. SARAL is the first satellite carrying on-board a Ka-band altimeter: AltiKa (35.75GHz). Over land-ice the Ka-band brings the advantage of being much less sensitive to volume scattering compared to conventional Ku-band (as seen in section 2).

The large AltiKa bandwidth (480 MHz) provides a better range resolution (**31cm** in Ka-band, versus **47cm** in Ku-band). Consequently, the footprint is reduced: **11 km diameter** (considering whole waveform), and around **4,5 km diameter** considering only a leading edge of 10 samples (pulse-limited footprint). Finally, the AltiKa PRF provides twice more elementary data than usual altimeters (40Hz rate in Ka-band versus 20Hz rate in Ku-band).

AltiKa operates exclusively in LRM. It is positioned on the same orbit as Envisat: 35-day repeat orbit, inclination of 98.54° and a mean altitude of 790km. The figure below shows a map of one year of AltiKa tracks over Antarctica.

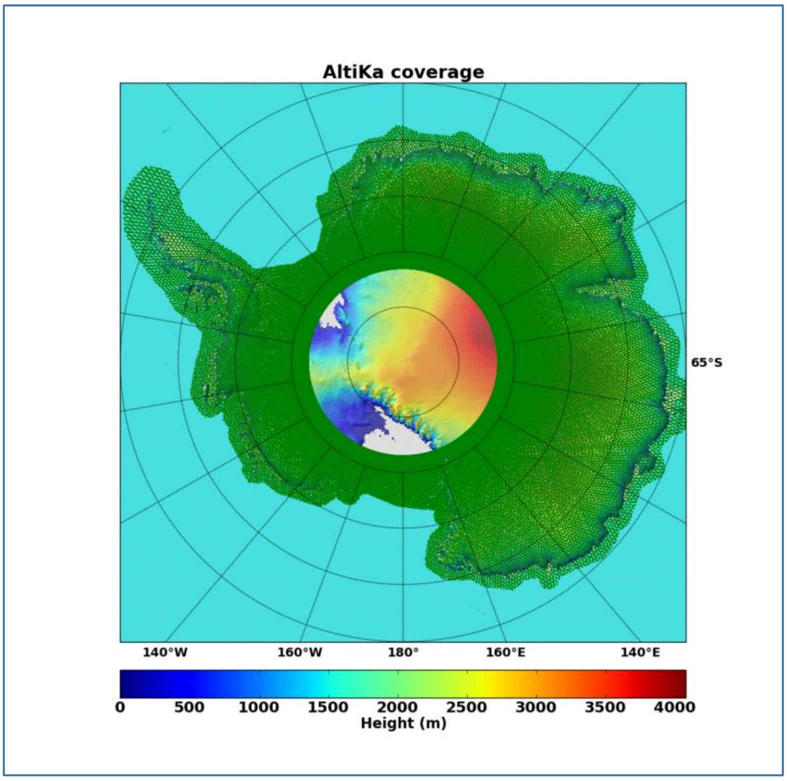


*Figure 3: One year of AltiKa tracks (green) over Antarctica*

More detailed information about the SARAL mission can be found in Steunou et al. [2015].

### 3.2.2. Measurements selected

Snow surface properties can change with meteorological conditions (temperature, wind, humidity…) and in case of snowfall events, bringing fresh snow at the surface. With a very dry atmosphere giving extremely rare rainfall events, Antarctica is considered as a desert. Over the plateau, snowfall rates do not exceed +6 to +8cm per year [Palerme et al., 2017]. The inland snow stays dry but is subject to seasonal metamorphism and compaction that occurs under temperature forcing, snow accumulation and wind driven process. That said, at a month time scale, surface snow properties are not expected to drastically change. Short time scale variations have been reported, but on extremely rare occasions [Lacroix et al., 2009].

For this study, to make a fair comparison between both missions and assuming that Antarctica snow properties do not change much over one month, only one AltiKa radar cycle is analysed, corresponding to 35 days of acquisitions around the time period of the Cryosat-2 acquisitions. Measurements analysed are acquired between November 10th and December 15th, 2014.

For this study we made the choice to retrieve the surface elevation starting from the L1 waveforms. It allowed us to run preliminary tests on the level-2 retracking and control the surface slope correction. The AltiKa waveforms used for this study come from the on-board processing. These waveforms have been retracked with an equivalent of the Threshold Peak Retracker (TPR), namely the Threshold First Maximum Retracker Algorithm (TFMRA) as described by Helm et al. [2014]. TPR and TFMRA have similar behaviours. These empirical retrackers provide the first sample that reaches the amplitude set by a threshold. Only major difference is that in TFMRA the waveform is smoothed beforehand maximum amplitude to reduce speckle noise effect. For AltiKa the TFMRA threshold is set to 50%. There are more details about the threshold choices in section 6.3. Note the epoch estimations from TFMRA should theoretically be close to the Sea-Ice retracker estimations, from the AltiKa official product, operating with a 50% threshold.

SARAL [Prandi and Debout, 2016] is regularly experiencing mispointing events since the beginning of the mission. The number of mispointing events has raised from September 2014 due to an increase in reaction wheel friction. In case of strong platform mispointing, the measured waveform can be dramatically distorted. This could lead to large retracking errors, in particular when using empirical retrackers such as TFMRA, ICE-1… as they do not account for the platform bad pointing. Therefore, based on the StarTracker platform angles (roll and pitch) provided by ISRO, AltiKa strong mispointing events are edited when mispointing is estimated greater than 0.0625 $deg^2$.

# 4. Topography of the three selected sites

## 4.1. Vostok

Cryosat-2 acquired around 10 000 measurements at 20Hz rate over Vostok area between November 18th and December 8th, 2014. The following figures show the location of the Cryosat-2 tracks acquired over Vostok area:

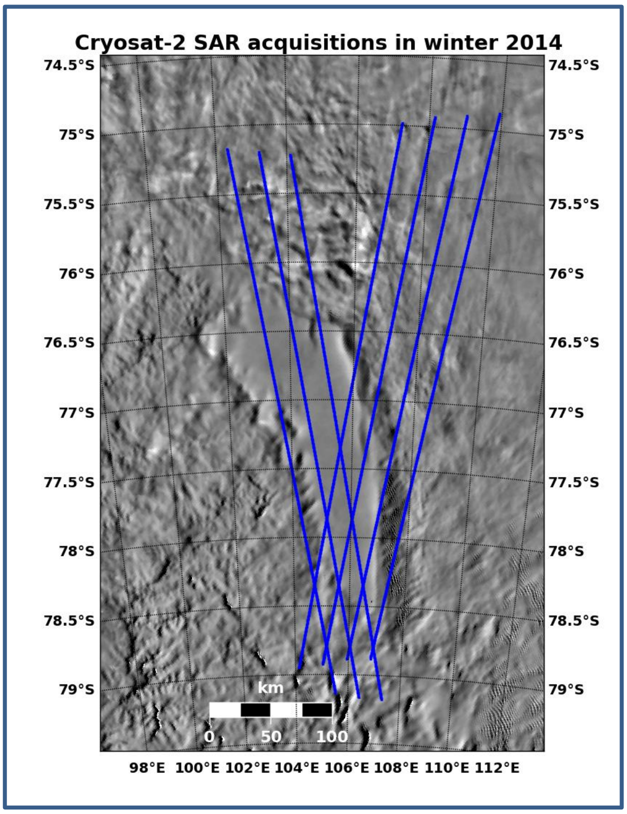


*Figure 4: Location of the Cryosat-2 SAR tracks over Vostok area in winter 2014 (blue). In the background, a surface morphology image from MODIS.*

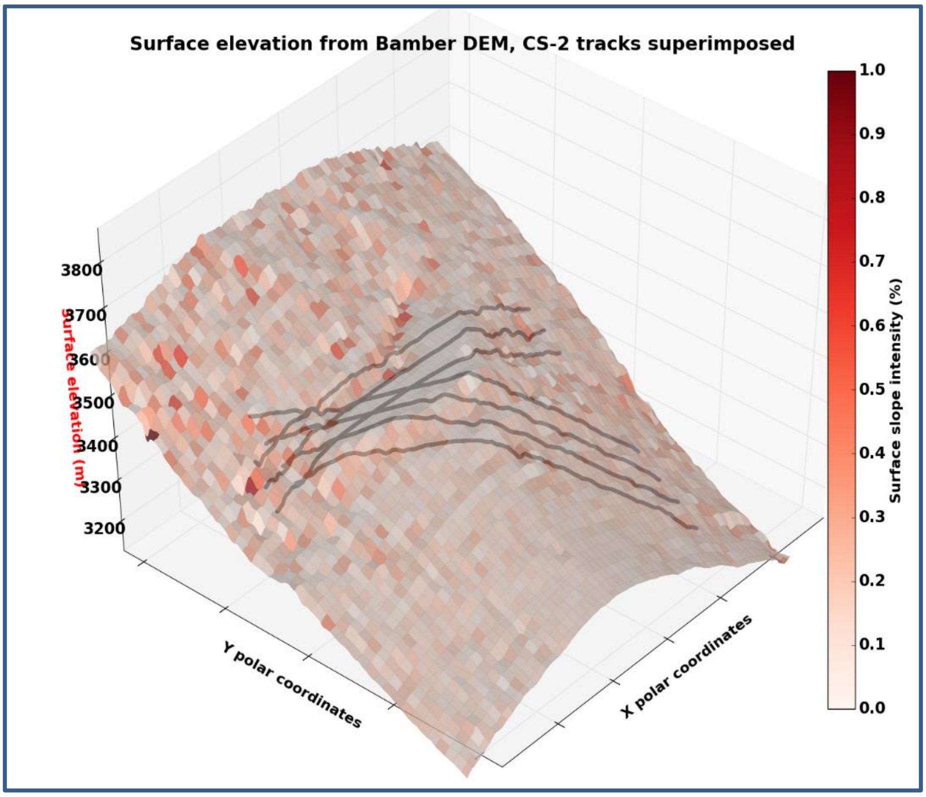


***Figure 5**: 3-dimensionnal representation of Vostok area from Bamber DEM [2009]. Cryosat-2 tracks are superimposed in dark blue. Pixel color gives the surface slope magnitude.*

Lake Vostok is the largest subglacial lakes known in Antarctica. Measuring 250 km long by 50 km wide at its widest point, it covers an area of 12 500 km2 and is located at an elevation of around 3 500 metres above sea level. This large area has the specificity to be remarkably flat. Surface has been reported very smooth, without the presence of sastrugi or others topographic features [Siegert, 2005; Ewert et al., 2012]. The surface smoothness is visible on the MODIS image previously displayed. These characteristics make it a unique calibration site over the Antarctica.

In addition, lake Vostok has an equilibrated local ice-mass balance. The mean surface elevation due to snow accumulation is **+6.24 cm/yr** [Ekaykin et al., 2004]. The mean vertical velocity of snow particle due to snow/firn densification is **-6.17 cm/yr** [Richter et al., 2014]. Analyses of GNSS data from 2001 to 2015 demonstrate that the surface is extremely stable over time, with a mean surface elevation rate of **+1mm/yr** [Richter et al., 2014] and **0mm/yr** [Schröder et al., 2017].

Nevertheless, the surface still presents a slight north–south slope, tilting 60m over a horizontal distance of around 250 km. Consequently, even if the surface is extremely flat (average slope of 0.025%), the slope-induced error in LRM still causes a POCA displacement of around 175m upslope and leads to bias the altimeter range of around 2cm (based on equation section 3.1.2).

Around Vostok area, the surface is characterized by a slope of around 0.2% to 0.3%, with a rougher topography compared to lake Vostok.

## 4.2. DOME-C

Cryosat-2 acquired around 2 500 measurements at 20Hz rate over DOME-C between November 18$^{th}$ and December 8$^{th}$, 2014. The following figures show the Cryosat-2 tracks acquired over the area. The red circle indicates the location of the Concordia research station.

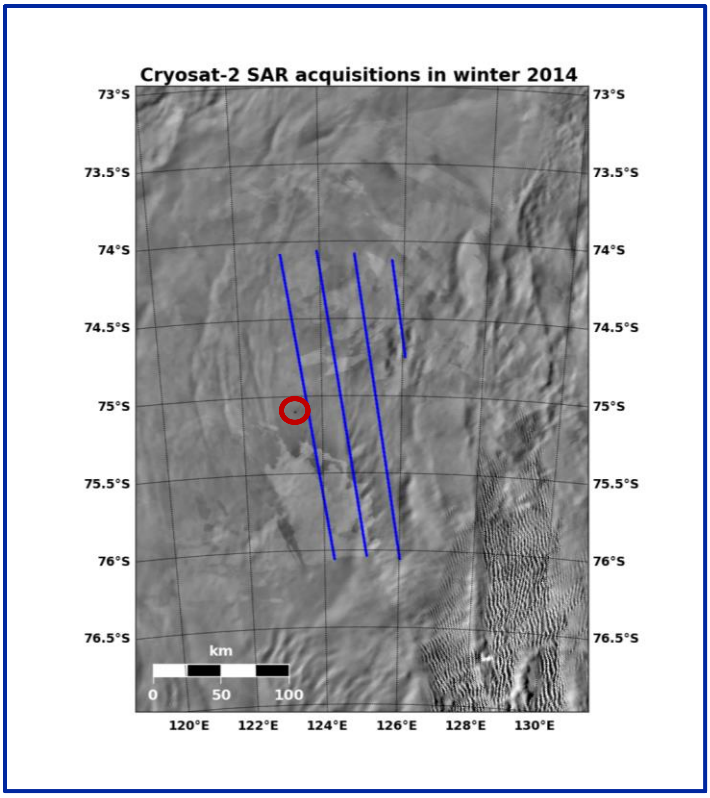


*Figure 6: Location of the Cryosat-2 SAR mode tracks over DOME-C in winter 2014 (blue). In the background, a surface morphology image from MODIS. Red circle indicates Concordia station location.*

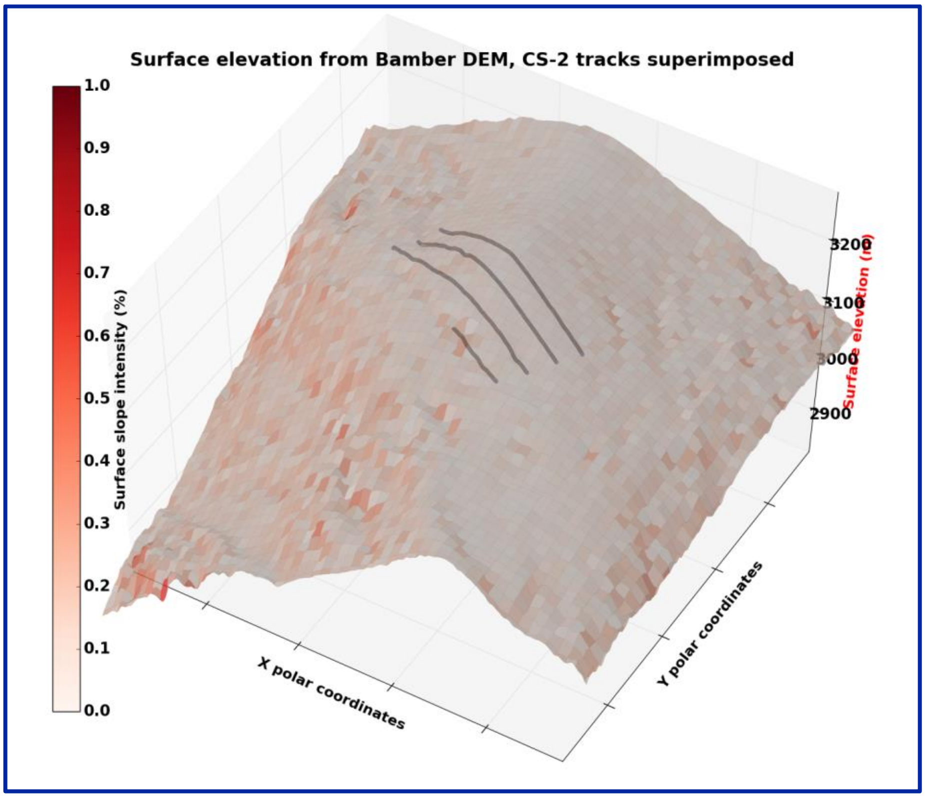


*Figure 7: 3-dimensionnal representation of DOME-C area from Bamber DEM [2009]. Cryosat-2 tracks are superimposed in dark blue. Pixel color gives the surface slope magnitude.*

Dome C, also known as Dome Concordia, is located at an elevation of 3 233 metres above sea level, is one of the few summits or "domes" of the Antarctic Ice Sheet. The snow surface is spatially homogeneous but rougher than over lake Vostok with the presence of sastrugi at the meter scale in horizontal and up to 10–20 cm in height.

The topography is relatively flat, from Bamber DEM the surface slope is 0.07% in average. In LRM this slope intensity still creates a POCA displacement of around 500 meters upslope and leads to bias the altimeter range of around 35 cm. (based on equations section 3.1.2)

## 4.3. SPIRIT (Terre Adélie)

Cryosat-2 acquired around 10 000 measurements at 20Hz rate over SPIRIT area between November 18th and December 8th, 2014. The following figures show the Cryosat-2 tracks acquired over the area. The coastal line is displayed in red color.

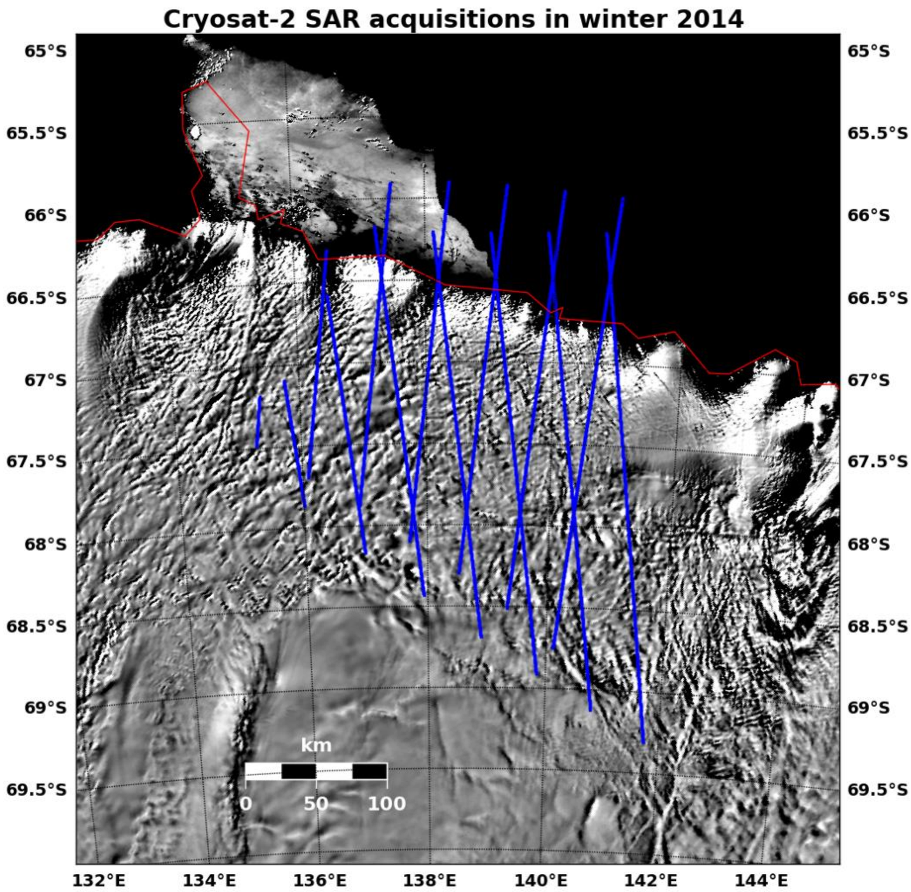


*Figure 8: Location of the Cryosat-2 SAR mode tracks over SPIRIT area in winter 2014 (blue). In the background, a surface morphology image from MODIS.*

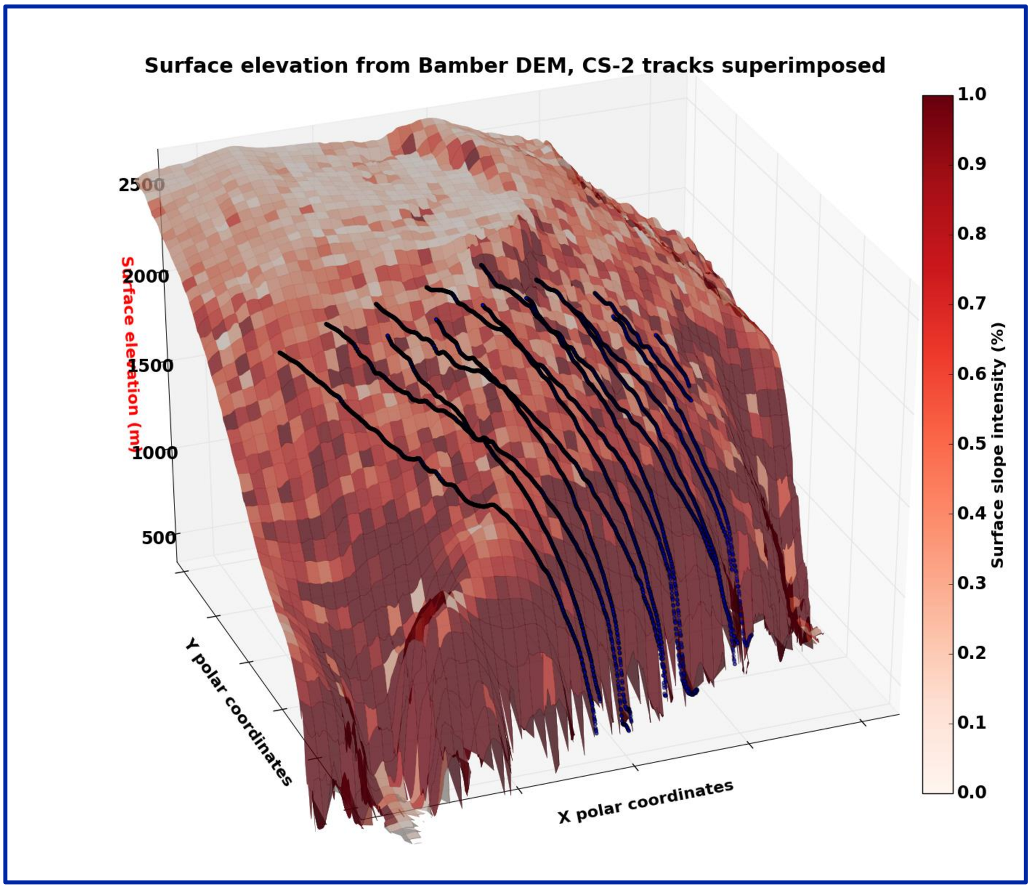


*Figure 9: 3-dimensionnal representation of SPIRIT area from Bamber DEM [2009]. Cryosat-2 tracks are superimposed in dark blue. Pixel's color give the surface slope magnitude.*

The final site is located over the Antarctica margins, in Terre Adélie, with very different characteristics than the two other sites. The satellite tracks sample a surface with an elevation varying sharply from around 2 000 meters to sea level. Consequently, surface is very steep and slope can reach several percents. At this magnitude, in LRM, POCA is shifted upslope by several kilometers (6 500 meters at 1% of slope), even outside of the antenna pattern for the steepest surfaces. The slope-induced error on the altimeter range can reach several decimeters (30 meters at 1% of slope).

The surface slope and the rugged topography complicate the interpretation of the altimeter signal. Multi-peak waveforms are frequently measured by the radar altimeter over the Antarctica margins. The difficulty is then to distinguish each peak and to localize their respective origin on the ground.

## 4.4. Selected sites for the study

The general purpose of the study is to assess the radar wave interaction with the snowpack at Ku/Ka crossovers. As previously described in sections 3.1.2, surface topography has a strong impact on the altimetry measure. It complexifies crossovers interpretation in two main ways:

- First, in LRM, the waveform shape is modified by the surface slope. The waveform trailing edge is specifically impacted, with an increase of its energy [Lacroix et al., 2007]. This effect is linked to the antenna pattern, and a same surface slope will act differently on AltiKa and Cryosat-2 waveform shape. In SAR mode this problem is currently not well quantified.

- Second, as described in section 3.1.2, the surface slope modifies the location of the POCA on-ground. In case of along-track slope, POCA location remains in the Doppler band in SAR mode, while it is shifted upslope within the radar footprint in LRM. To be correctly interpreted, crossover analysis must be performed at POCA locations, where surface elevation is estimated, not at the satellite nadir. With the knowledge of the surface topography over the radar footprint, it is theoretically possible to estimate the POCA location in LRM and SAR [Bamber, 1994], and therefore possible to find exact crossover points. Nevertheless, Antarctica topography is not perfectly well known and large uncertainties remain.

Error on the altimeter range and on the POCA relocation varies with the surface slope intensity, as presented in the table below for Croysat-2 (top) and AltiKa (bottom).

| Slope (%) | 0.01 | 0.025 | 0.1 | 0.25 | 0.5 | 1 | 1.5 | 2 |
|---|---|---|---|---|---|---|---|---|
| Slope (°) | 0.006 | 0.014 | 0.057 | 0.143 | 0.286 | 0.573 | 0.859 | 1.146 |
| Error on the altimeter range (m) | 0.003 | 0.02 | 0.33 | 2.03 | 8.14 | 32.55 | 73.23 | 130.17 |
| POCA displacement on-ground (m) | 65 | 163 | 651 | 1 627 | 3 255 | 6 510 | 9 764 | 13 018 |

Cryosat-2

| Slope (%) | 0.01 | 0.025 | 0.1 | 0.25 | 0.5 | 1 | 1.5 | 2 |
|---|---|---|---|---|---|---|---|---|
| Slope (°) | 0.006 | 0.014 | 0.057 | 0.143 | 0.286 | 0.573 | 0.859 | 1.146 |
| Error on the altimeter range (m) | 0.004 | 0.02 | 0.35 | 2.22 | 8.88 | 35.53 | 79.96 | 142.12 |
| POCA displacement on-ground (m) | 71 | 178 | 710 | 1 777 | 3 554 | 7 108 | 10 661 | 14 215 |

AltiKa

*Figure 10: Based on equations given in 3.1.2, LRM slope-induced errors considering Cryosat-2 nominal altitude, 730km, (top) and AltiKa nominal altitude, 800km (bottom). Same errors in SARM for the across-track slope only.*

Consequently, to discriminate volume scattering effect from topography effect, two sites are selected for this study, presenting relative flat and smooth topography:

- **Lake Vostok:** The "ideal" site, reported very smooth, with an average slope of 0.025%. Measurements are geographically selected over the lake thanks to a dedicated shapefile generated for the study.

- **DOME-C:** Probably not as smooth as lake Vostok, but relatively flat with an average slope of 0.07% (from Bamber DEM)

The following figures show the Cryosat-2 and AltiKa track locations over the two selected sites for the study:

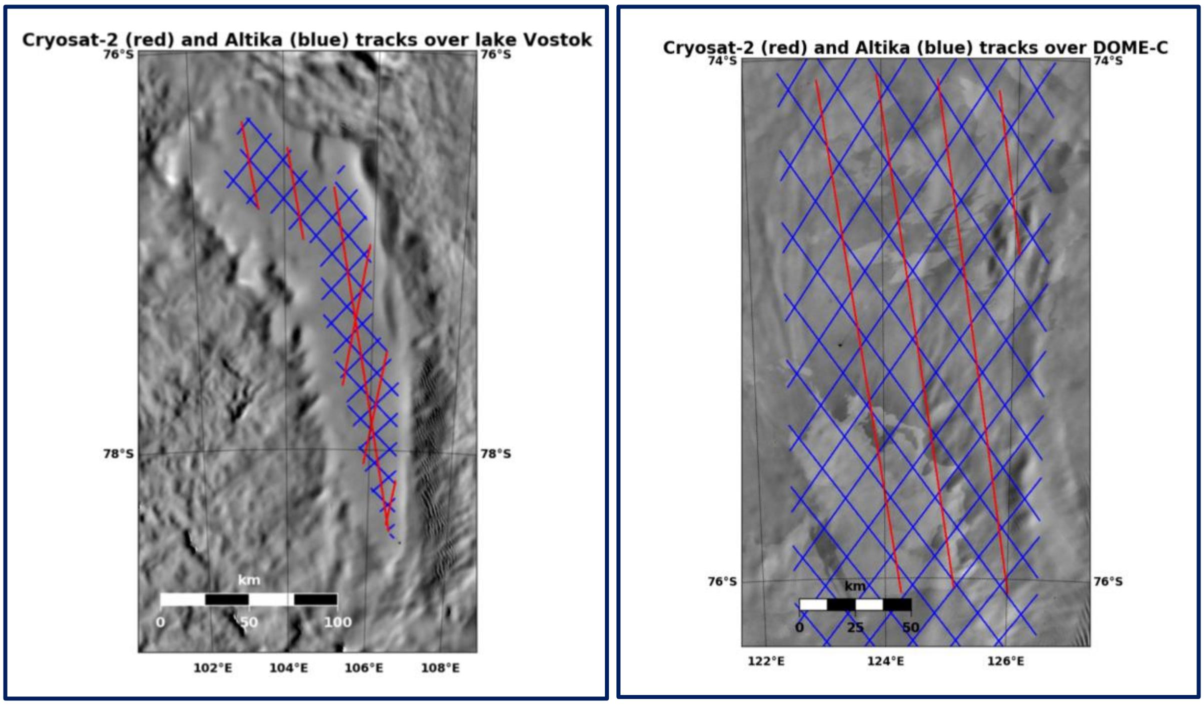


*Figure 11: Location of the Cryosat-2 SAR mode (red) and AltiKa (blue) tracks over the two selected sites for the WP5 study: lake Vostok (left) & DOME-C (right)*

Finally, considering that surface is flat, no surface slope corrections are applied. Crossover analyses are performed at nadir location of measurements.

FORM-NT-GB-7-1

# 5. Waveform analysis at crossovers

## 5.1. Methodology

The waveform analysis at crossover is performed following these processing steps:

- Find the two closest measurements at each Altika/Cryosat-2 crossovers located on the selected sites.
- To precisely analyze waveform shape, the waveform speckle noise is reduced by averaging individual measurements. Mean waveforms are generated by averaging 2 seconds of acquisition for both missions, around the crossover point (+/- 1s). This corresponds to 40 individual measurements at 20Hz rate for Cryosat-2 and 80 individual measurements at 80Hz rate for AltiKa. Individual waveforms are normalized before aggregation.
- Shift the leading edges for both missions to superimpose them with the aim to make the comparison more comprehensible. As range gate resolution differs between missions (31cm Altika vs 47cm Cryosat-2), range gates are converted to time delays beforehand to enable a consistent comparison.

Only crossovers distant by less than 7 days are kept for the study. During the past meetings of the project, the mean waveforms presented were generated from 4 seconds of averaging. We decided to lower the averaging time, considering that 2 seconds of acquisition are enough to provide smoothed waveforms. In addition, this leads to a better representation of the signal measured at crossover points.

The waveform position may change quickly in case of tracker instability. For such situations, the mean waveform can be distorted (leading edge inclination, trailing edge more powerful), and this can lead to wrong interpretations of the signal. To ensure the study consistency, the waveform stability within the window analysis was beforehand checked. The radargrams showing the 2 seconds of acquisitions are displayed hereafter.

This section presents two analyzes:

- Comparison of AltiKa and Cryosat-2 waveforms at crossovers (section 5.2)
- Comparison of mean oceanic and ice-sheet waveforms (section 5.3)

The results are then discussed on the following conclusion (section 5.4).

A last analyze showing a comparison of Cryosat-2 waveforms at crossovers, between ascending/descending tracks, is finally presented (section 5.5).

## 5.2. Cryosat-2 / AltiKa crossovers

### 5.2.1. First crossover over lake Vostok

The figure below shows the location of a first crossover located over lake Vostok. The Cryosat-2 (red color) and AltiKa (blue color) measurements displayed the 2 seconds of acquisition averaged to build mean waveforms as presented below. Measurements have been acquired respectively on November 28th and 29th for **AltiKa** and **Cryosat-2** missions, with approximately 35 hours of time offset.

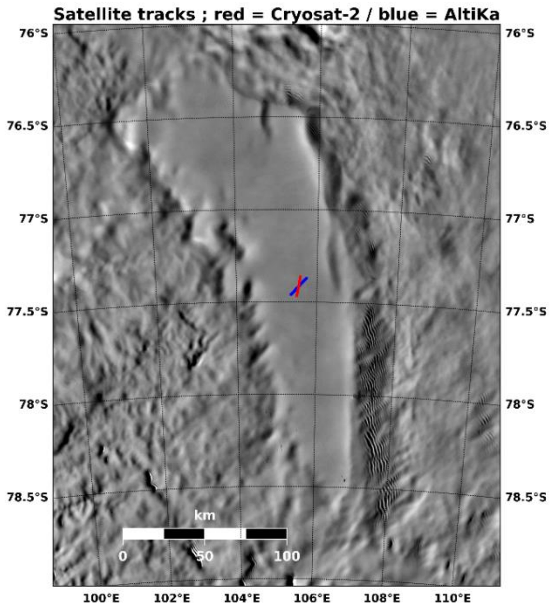


*Figure 12: Location of the Cryosat-2 (red) and AltiKa (blue) measurements averaged to build mean waveforms as displayed below.*

The following figure shows the individual and mean waveforms at crossovers: LRM AltiKa (blue color), Cryosat-2 LRM (green color), Cryosat-2 SARM (red color).

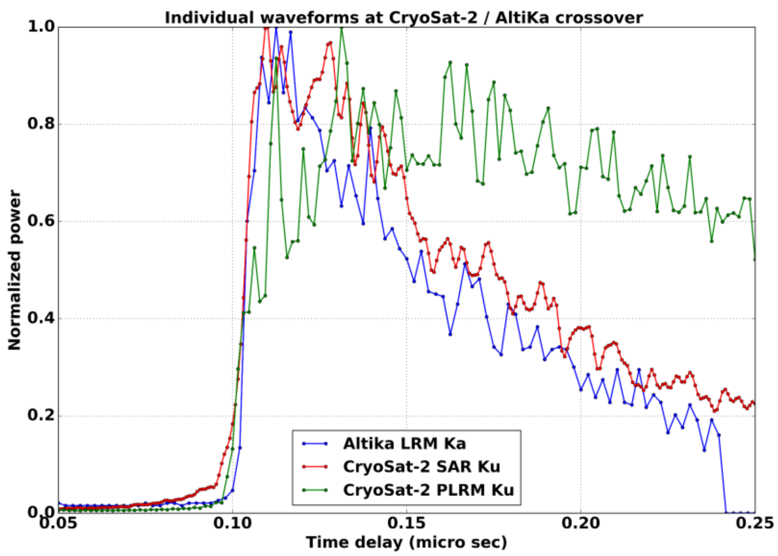


*Figure 13: Individual waveforms at the first crossover studied over lake Vostok: AltiKa LRM (blue), Cryosat-2 P-LRM (green) & Cryosat-2 SAR (red)*

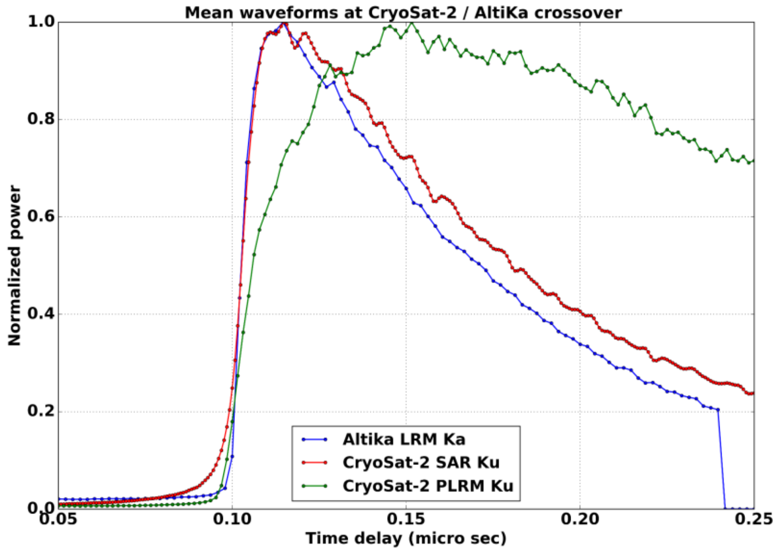


***Figure 14: Mean waveforms at the first crossover studied over lake Vostok: AltiKa LRM (blue), Cryosat-2 P-LRM (green) & Cryosat-2 SAR (red)***

The following figure shows the radargrams at crossover for the Altika and Cryosat-2 missions. It illustrates the tracker stability for the aggregated acquisitions.

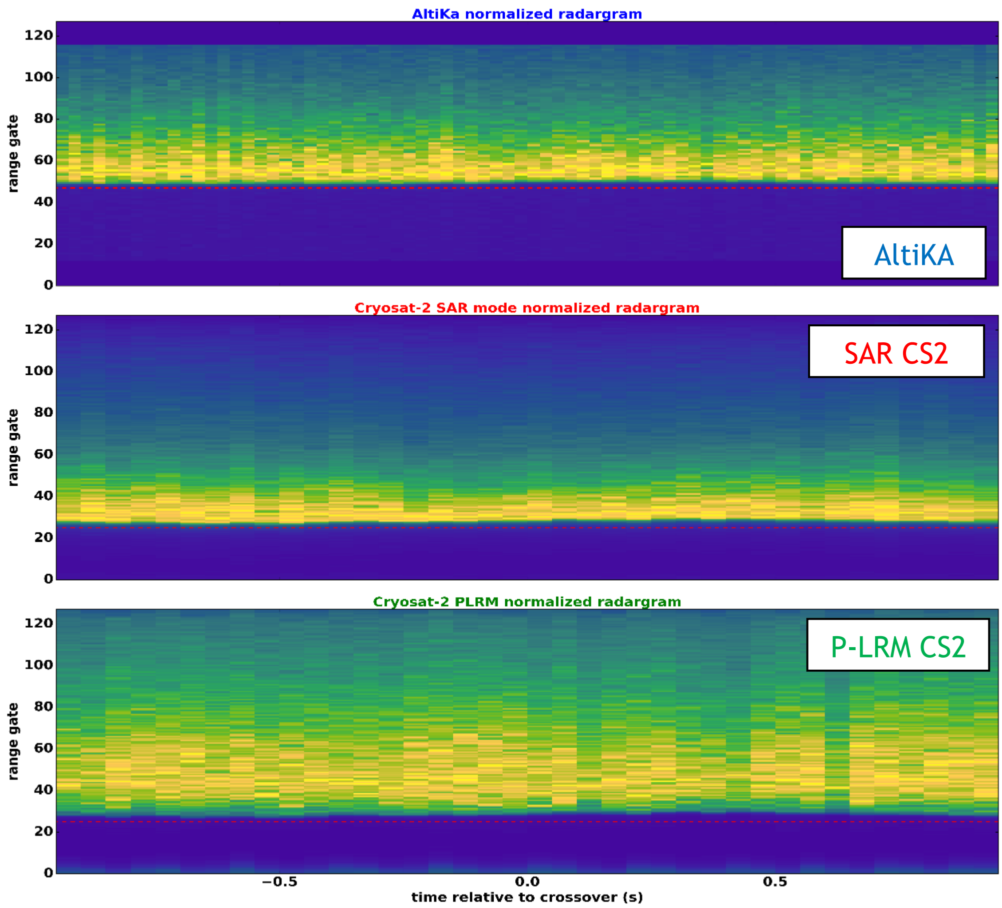


***Figure 15: Individual waveforms along the 2 seconds satellite tracks for AltiKa (top), SAR Cryosat-2 (middle), P-LRM Cryosat-2 (bottom)***

FORM-NT-GB-7-1

### 5.2.2. Second crossovers over lake Vostok

The figure below shows the location of a second crossover located over lake Vostok. The Cryosat-2 (red color) and AltiKa (blue color) measurements displayed 2 seconds of acquisitions averaged to build mean, smoothed waveforms. Measurements have been acquired respectively on November 19th for **AltiKa** and November 25th **Cryosat-2** missions, with approximately 6 days of time offset.

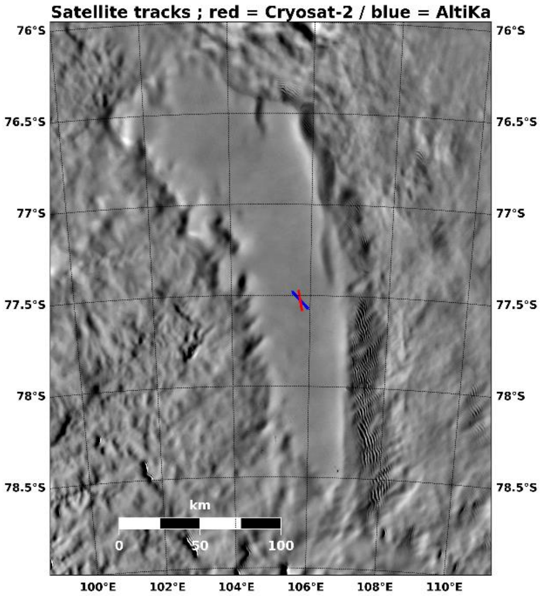


***Figure 16: Location of the Cryosat-2 (red) and AltiKa (blue) tracks for the second crossover analysed, corresponding to 2 seconds of acquisitions***

The following figure shows the individual and mean waveforms at crossovers: LRM AltiKa (blue color), Cryosat-2 LRM (green color), Cryosat-2 SARM (red color).

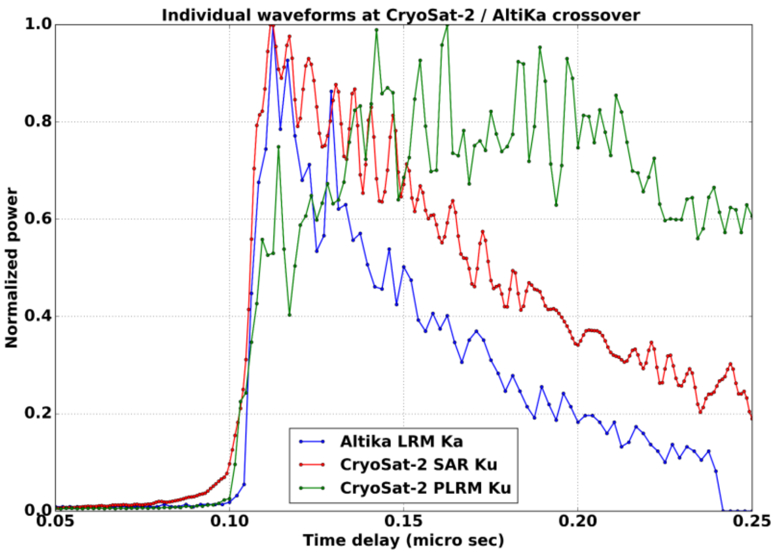


***Figure 17: Individual waveforms at the second crossover studied over lake Vostok: AltiKa LRM (blue), Cryosat-2 P-LRM (green) & Cryosat-2 SAR (red)***

*FORM-NT-GB-7-1*

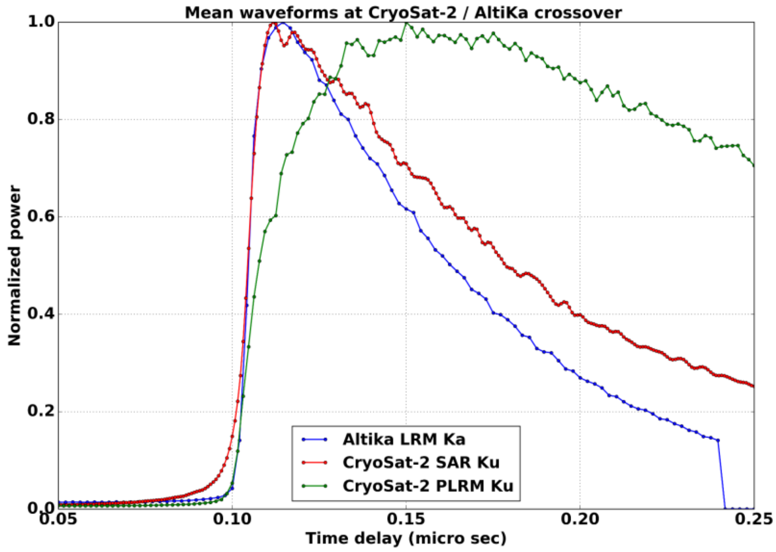


*Figure 18: Mean waveforms at the second crossover studied over lake Vostok: AltiKa LRM (blue), Cryosat-2 P-LRM (green) & Cryosat-2 SAR (red)*

The following figure shows the radargrams at crossover for the Altika and Cryosat-2 missions. It illustrates the tracker stability for the aggregated acquisitions.

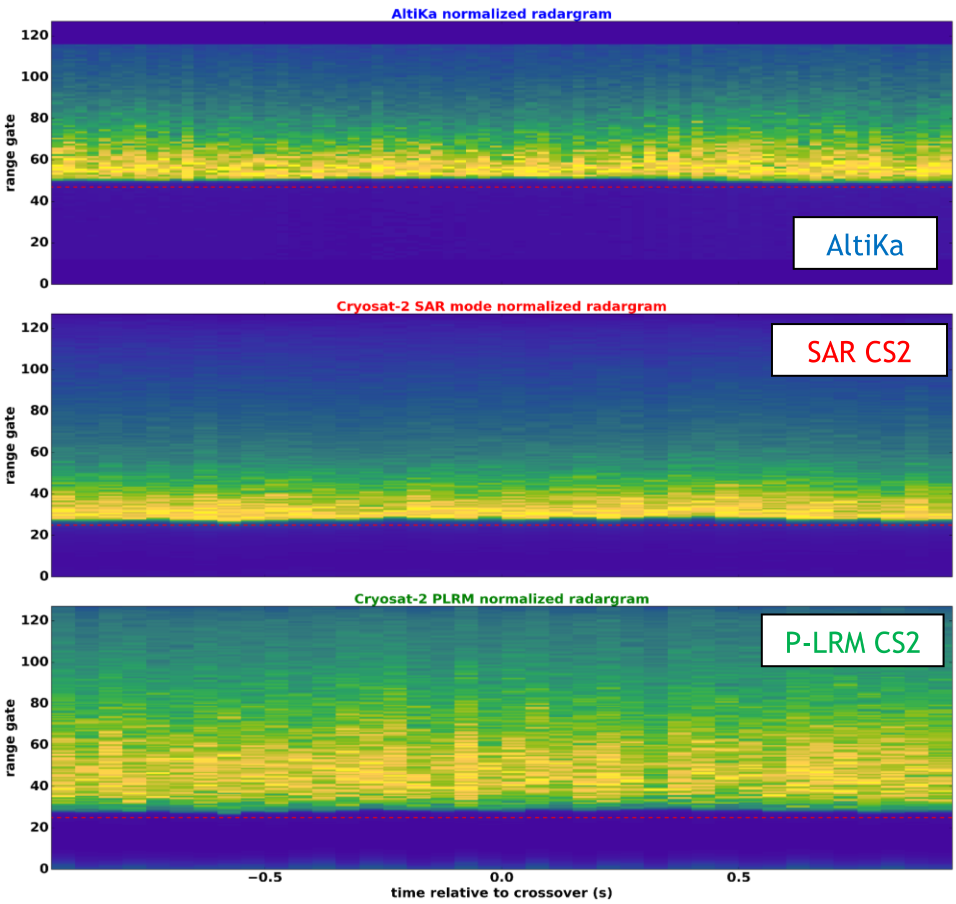


*Figure 19: Individual waveforms along the 2 seconds satellite tracks for AltiKa (top), SAR Cryosat-2 (middle), P-LRM Cryosat-2 (bottom).*

### 5.2.3. Third crossovers over lake Vostok

The figure below shows the location of a third crossover located over lake Vostok. The Cryosat-2 (red color) and AltiKa (blue color) measurements displayed 2 seconds of acquisitions averaged to build mean, smoothed waveforms. Measurements have been acquired respectively on November 22th for **AltiKa** and November 28th **Cryosat-2** missions, with approximately 6 days of time offset.

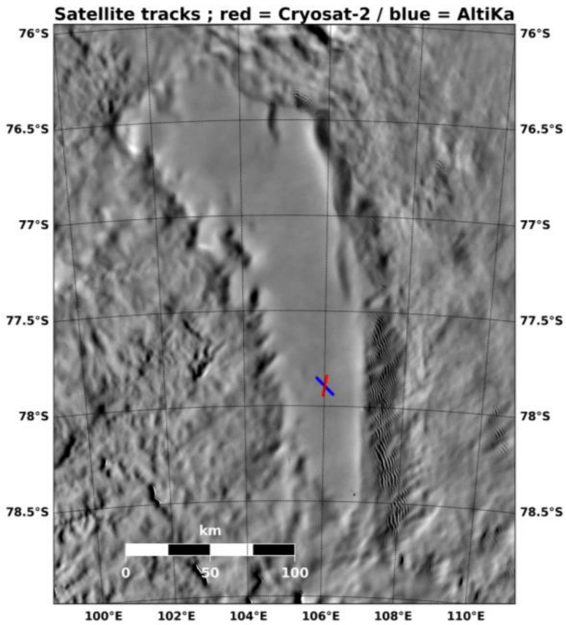


*Figure 20: Location of the Cryosat-2 (red) and AltiKa (blue) tracks for the third crossover analysed, corresponding to the 2 seconds of acquisitions analysed*

The following figure shows the individual and mean waveforms at crossovers: LRM AltiKa (blue color), Cryosat-2 LRM (green color), Cryosat-2 SARM (red color):

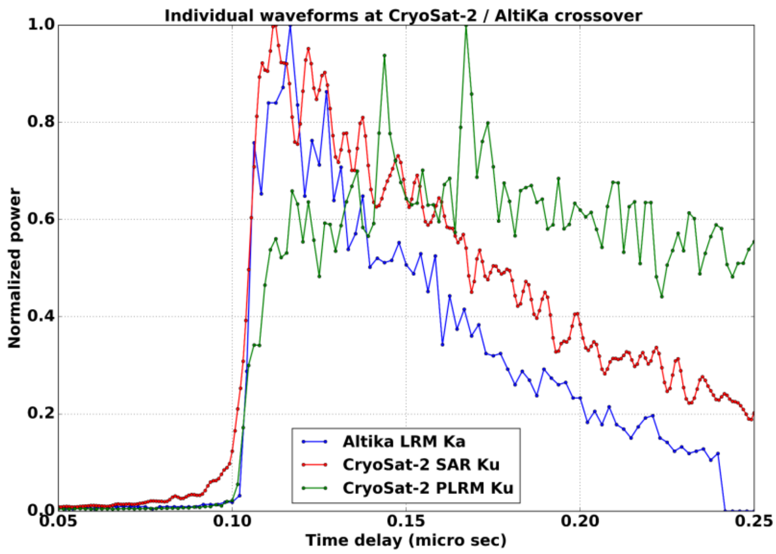


*Figure 21: Individual waveforms at the third crossover studied over lake Vostok: AltiKa LRM (blue), Cryosat-2 P-LRM (green) & Cryosat-2 SAR (red)*

FORM-NT-GB-7-1

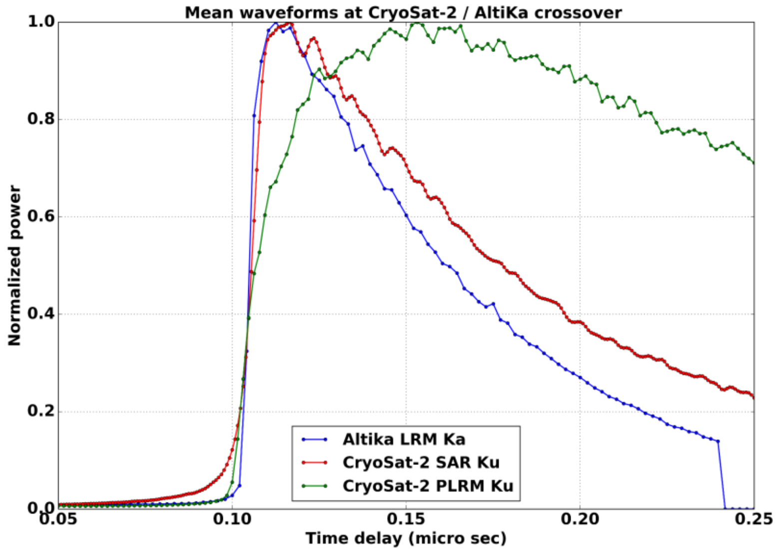


*Figure 22: Mean waveforms at the third crossover studied over lake Vostok: AltiKa LRM (blue), Cryosat-2 P-LRM (green) & Cryosat-2 SAR (red)*

The following figure shows the radargrams at crossover for the Altika and Cryosat-2 missions. It illustrates the tracker stability for the aggregated acquisitions.

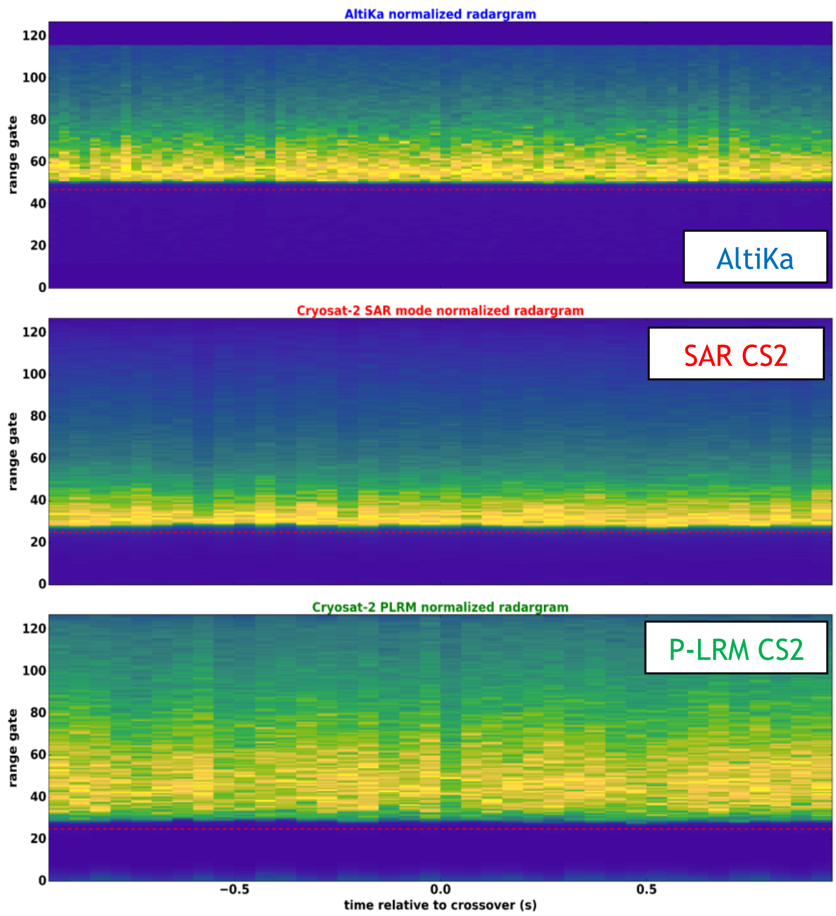


*Figure 23: Individual waveforms along the 2 seconds satellite tracks for AltiKa (top), SAR Cryosat-2 (middle), P-LRM Cryosat-2 (bottom)*

### 5.2.4. Crossover over DOME-C

The figure below shows the location of a first crossover located over DOME-C. The Cryosat-2 (red color) and AltiKa (blue color) measurements displayed 2 seconds of acquisitions averaged to build mean, smoothed waveforms. Measurements have been acquired respectively on December 8th and 7th for **AltiKa** and **Cryosat-2** missions, with approximately 14 hours of time offset.

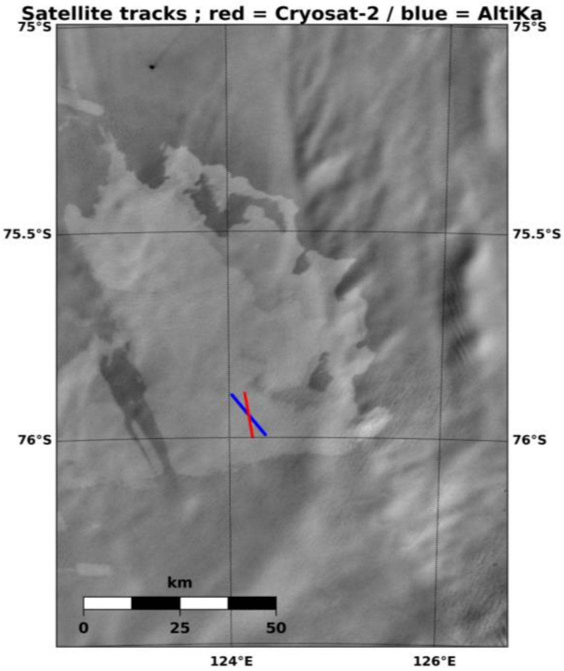


***Figure 24: Location of the Cryosat-2 (red) and AltiKa (blue) tracks for the crossover analysed over DOME-C, corresponding to 2 seconds of acquisitions analysed***

The following figure shows the individual and mean waveforms at crossovers: LRM AltiKa (blue color), Cryosat-2 LRM (green color), Cryosat-2 SARM (red color):

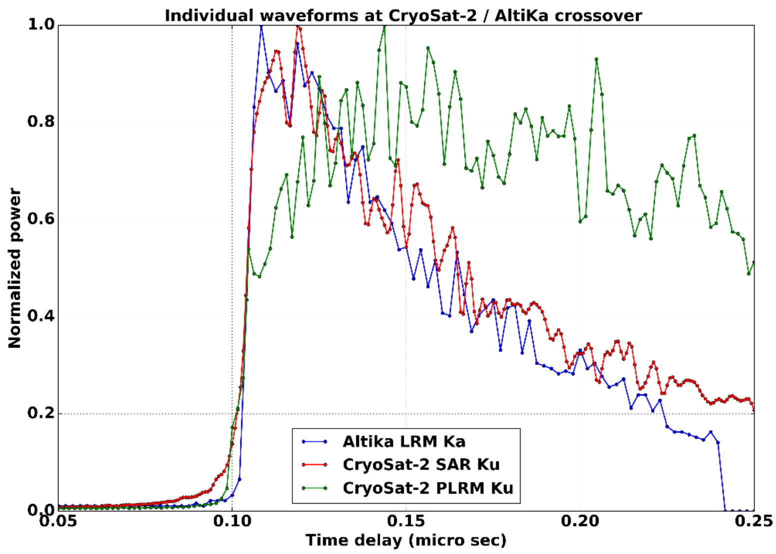


***Figure 25: Individual waveforms at the DOME-C crossover: AltiKa LRM (blue), Cryosat-2 LRM (green) & Cryosat-2 SAR (red)***

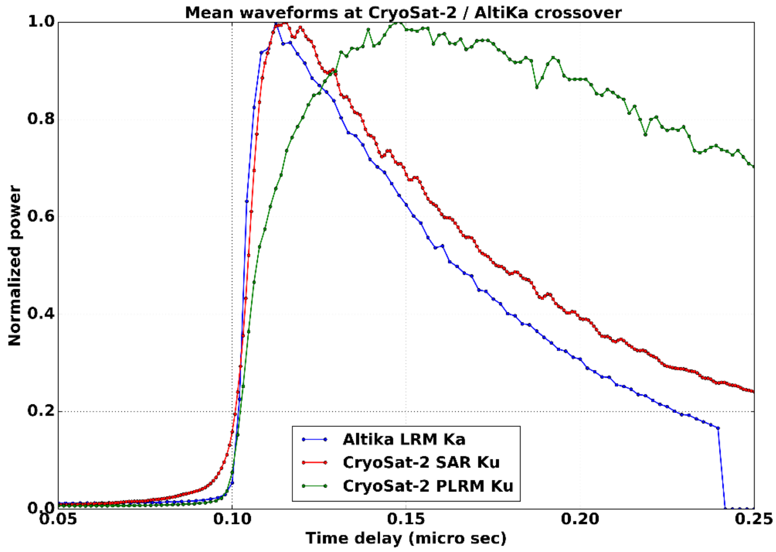


*Figure 26: Mean waveforms at the DOME-C crossover: AltiKa LRM (blue), Cryosat-2 LRM (green) & Cryosat-2 SAR (red)*

The following figure shows the radargrams at crossover for the Altika and Cryosat-2 missions. It illustrates the tracker stability for the aggregated acquisitions.

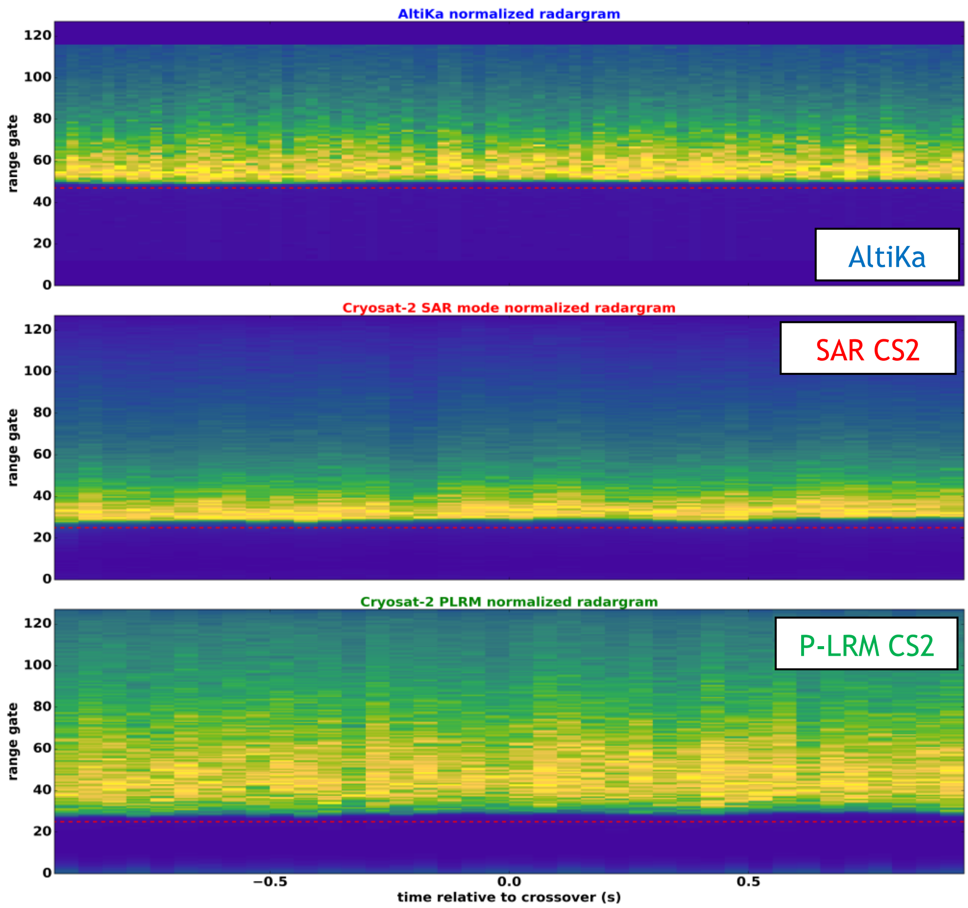


*Figure 27: Individual waveforms along the 2 seconds satellite tracks for AltiKa (top), SAR Cryosat-2 (middle), P-LRM Cryosat-2 (bottom)*

## 5.3. Comparison of ice-sheets and oceanic waveforms

To better understand the volume scattering effect on LRM/SAR modes and Ku/Ka bands, this section presents a comparison of oceanic and ice-sheet waveforms. Over ocean, the altimeter signal is only reflected by the water surface. The waveform shape distortion observed over ice sheet, induced by the sub-surface signal, will hence be directly visible. As lake Vostok surface is reported very smooth (see section 4.1), the objective of the study is to make a comparison with oceanic measurements acquired where the oceanic surface is the smoothest, under calm sea state conditions.

**Mean oceanic waveforms** have been selected over central Pacific and computed for SWH=1m (± 20cm) with epoch positioned at the mission reference range gate (± 0.1 range gate). For AltiKa, **1498** individual waveforms have been aggregated. For SAR and P-LRM Cryosat-2, respectively **425** and **377** individual waveforms have been aggregated. The mean waveform computed for the second lake Vostok crossover (section 5.2.2) is set arbitrarily as the reference ice-sheet waveform. We must note that the oceanic and ice-sheet waveforms have been artificially aligned in order to compare their leading edges.

The following figures show the mean ice-sheet and oceanic waveforms for AltiKa (top), Cryosat-2 P-LRM (middle) and Cryosat-2 SARM (bottom):

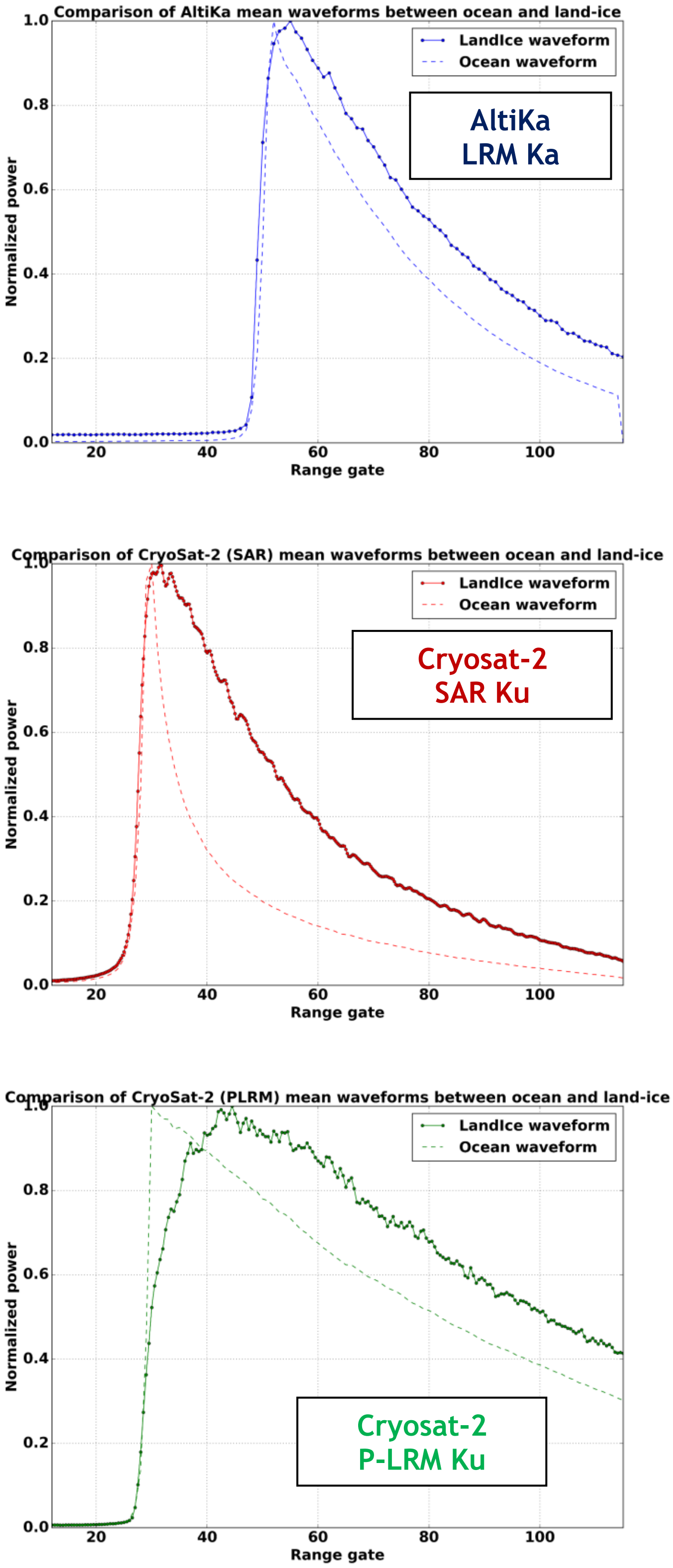


***Figure 28: Mean oceanic (dotted lines) and ice-sheet (solid lines) waveforms for LRM Ka AltiKa (top), SAR Ku Cryosat-2 (middle), P-LRM Ku Sentinel-3A (bottom)***

## 5.4. Conclusions

The study of the waveform shape at Ku/Ka crossovers and the comparison with oceanic measurements bring the following main conclusions:

**Cryosat-2 P-LRM Ku band**

For acquisitions over ice sheet in LRM/P-LRM **in Ku band**, the waveform leading edge (green) is distorted by the volume scattering effect, particularly from mid-power. The waveform reaches its maximum power approximately 10 to 15 range gates later compared to an oceanic measurement. This has been previously stated by other studies [Ridley & Partington, 1988 ; Femenias et al., 1993; Davis, 1997].

The leading edge of the waveform is directly sensitive to the uppermost part of the snowpack and therefore to its temporal and spatial variability [Remy & Parouty, 2009]. This complicates the estimation of a stable, repeatable, surface elevation when using an empirical retracker based on a static threshold. Consequently, Davis [1997] recommended to use a low threshold for obtaining a repeatable estimate of the ice-sheet elevation, best suited for elevation-change detection. From his work, a 10% threshold level produces the most repeatable elevation estimates and a 20% threshold provides a reasonable estimate of the true ice-sheet elevation in an average sense.

**AltiKa LRM Ka band**

In contrast, the AltiKa leading edge waveform measured over ice sheet remains visually steep. At least as steep as over ocean. This would indicate that the leading edge is generated by backscattered energy coming from the top layer of the snowpack, corresponding most probably to the snow/air interface. This is consistent with the theory, stating that the snow scattering coefficient increases from Ku to Ka band. Following this, the waveform energy should originate primarily from the surface. Consequently, the measure should be less sensitive to variations of subsurface snow properties. We expect it will provide better repeatable estimations than measure in Ku band.

Nevertheless, the volume scattering effect is clearly visible when comparing oceanic and ice-sheet waveforms (Figure 28). Over ice sheet, the upper part of the leading edge is slightly bended, and the waveform is more "volumic". This proves that a part of the Ka-band signal penetrates the snowpack and is backscattered by internal layers and/or snow grains.

**SAR Ku band**

As observed with AltiKa, the waveform leading edge of the ice sheet acquisitions remains visually steep, at least until 80% of maximum power. This was not expected in a first approach, as the LRM/P-LRM Ku band waveform leading edge is strongly distorted. The difference is explained by the specific sampling of the SAR altimetry measure. On the contrary to P-LRM, there is an exponential decrease of the surface area covered on ground by each range gate. Hence, oppositely to LRM / P-LRM, the delayed energy coming from the snowpack interior does not bring enough power to distort the waveform leading edge.

However, the volume scattering effect clearly impacts the trailing edge, much more volumic compared to ocean.

In Ku band, the leading edge stability observed in SAR mode looks clearly as a strong advantage compared to LRM / P-LRM. We expect that the estimations retrieved from the SAR waveforms will be less sensitive to volume scattering and its temporal/spatial variations. At least if the epoch position is searched low enough in the leading edge, below 80% of maximum power.

## 5.5. Comparison of ascending/descending tracks of Croysat-2

It is now well-known that the interaction between azimuthally anisotropic features of the firn and the altimeter polarization direction affects the backscatter coefficient measured by radar altimeters [Legrésy et al.,1999 ; Rémy et al., 2012]. As a side effect, strong differences of the surface elevation estimated can be observed at crossovers, depending on the retracking algorithm employed [Armitage et al, 2014].

Over the smooth surface of lake Vostok and relatively smooth surface of DOME-C, there is theoretically no topographic features which could create such effect. Nevertheless, this study is an opportunity to check and verify this assumption. As done for the AltiKa/Cryosat-2 crossovers, mean ice sheet waveforms are computed between ascending and descending tracks of Cryosat-2 by averaging 2 seconds of acquisition.

The figure below shows the location of a crossover located over lake Vostok. The Cryosat-2 ascending (blue color) and descending (cyan color) measurements displayed 2 seconds of acquisition averaged to build mean, smoothed waveforms. Measurements have been acquired respectively on December 25$^{th}$ and 28$^{th}$ for **ascending and descending tracks.**

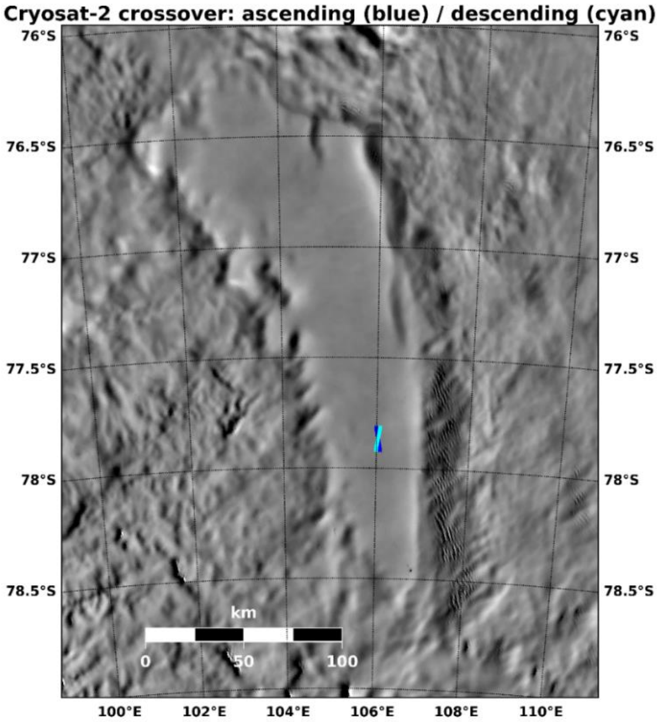


***Figure 29: Location of the ascending (blue) and descending (cyan) Cryosat-2 tracks, corresponding to 2 seconds of acquisition***

The following figure shows the mean waveforms at crossover in P-LRM (top) and SAR mode (bottom), for the ascending (blue) and descending tracks (cyan)

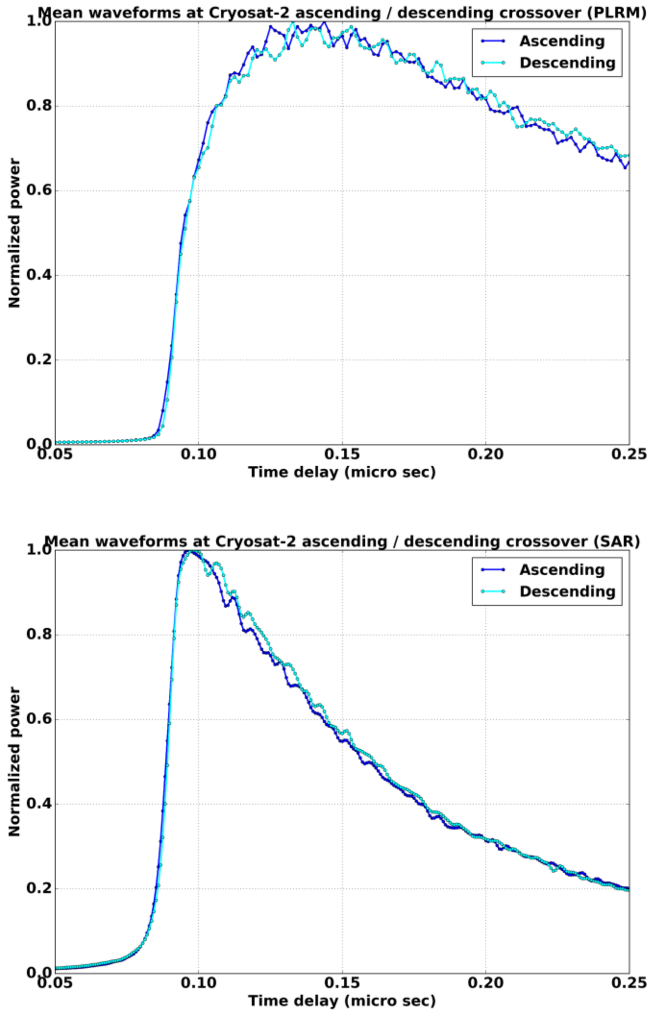


***Figure 30: Mean Cryosat-2 waveforms for ascending (blue) and descending (cyan) tracks, computed by averaging 2 seconds of acquisition at crossovers in P-LRM (top) and SAR mode (bottom)***

⇨ As expected the comparison performed over lake Vostok shows no particular differences between ascending and descending signals.

## 6. Ice sheet elevation at crossovers

### 6.1. Selected crossovers

Surface elevation estimated from Cryosat-2 and AltiKa measurements are now compared at crossovers, over the two selected sites of lake Vostok and DOME-C (see section 4.4). There are respectively 42 and 50 crossovers over lake Vostok and Dome-C with the selected data. The following maps display the crossovers location (yellow color):

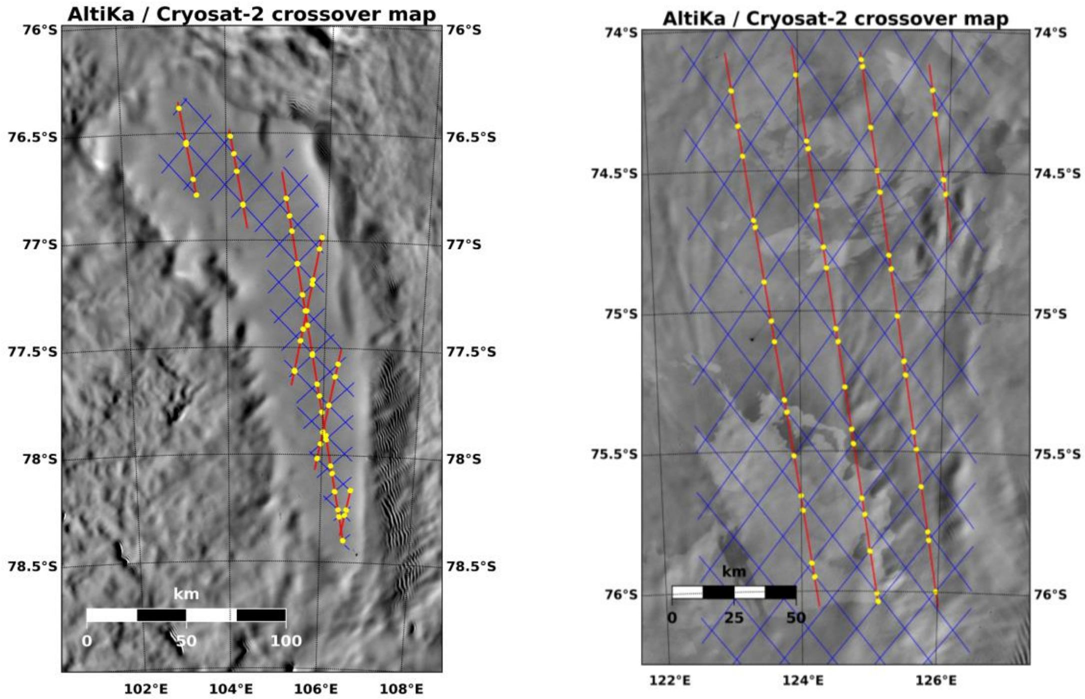


*Figure 31: Crossover maps between AltiKa (blue) and Cryosat-2 (red) missions over lake Vostok (left) and Dome-C (right). Yellow dots show the crossover locations.*

## 6.2. Surface elevation computation at crossover

The ice sheet height estimation is calculated as the difference between the orbit altitude and the altimeter range estimation, plus various conventional corrections due to ionospheric and tropospheric delays, solid Earth and pole tides and instrumental biases. For the AltiKa mission, an intercalibration bias of **+4.5cm,** computed from oceanic Cal/Val studies at CLS, is added to the surface elevation [Prandi et al., 2015]. In addition, as previously mentioned section 3.2, strong mispointing events of AltiKa are edited when mispointing is greater than 0.0625 $deg^2$ to avoid inconsistent estimations.

To make the comparison as accurate as possible, surface elevation estimated from both missions is interpolated at the exact on-ground crossover point. Here, we assume that surface on-ground is flat (see section 4) and therefore we do not relocate the measurements. First step is to project the altimetry longitudinal and latitudinal measurement coordinates in south polar stereographic coordinates (EPSG 3031). The two-dimensional cartesian coordinate plane simplifying the following computations. Second step consists in identifying a co-located point in space by using a fast nearest neighbor searches algorithm k-d tree [Bentley, 1975]. Nominally, each altimetry measurement is separated by approximately 300 meters (Cryosat-2) and 150 meters (AltiKa) on-ground. Measurement locations are then oversampled on-ground, along the track, to create a **50cm spatial sampling.** Surface elevation, beforehand slightly smoothed (see

**Figure 33**), is linearly interpolated at this 50cm sampling. This allows to determine a crossover point where measurements are separated by less than 1 meter on-ground.

The following figures 32 & 33 illustrate the computations performed to retrieve surface elevation at crossovers. The figure 32 shows the oversampled polar coordinates of Cryosat-2 (blue) and AltiKa (green) tracks in the (X,Y):

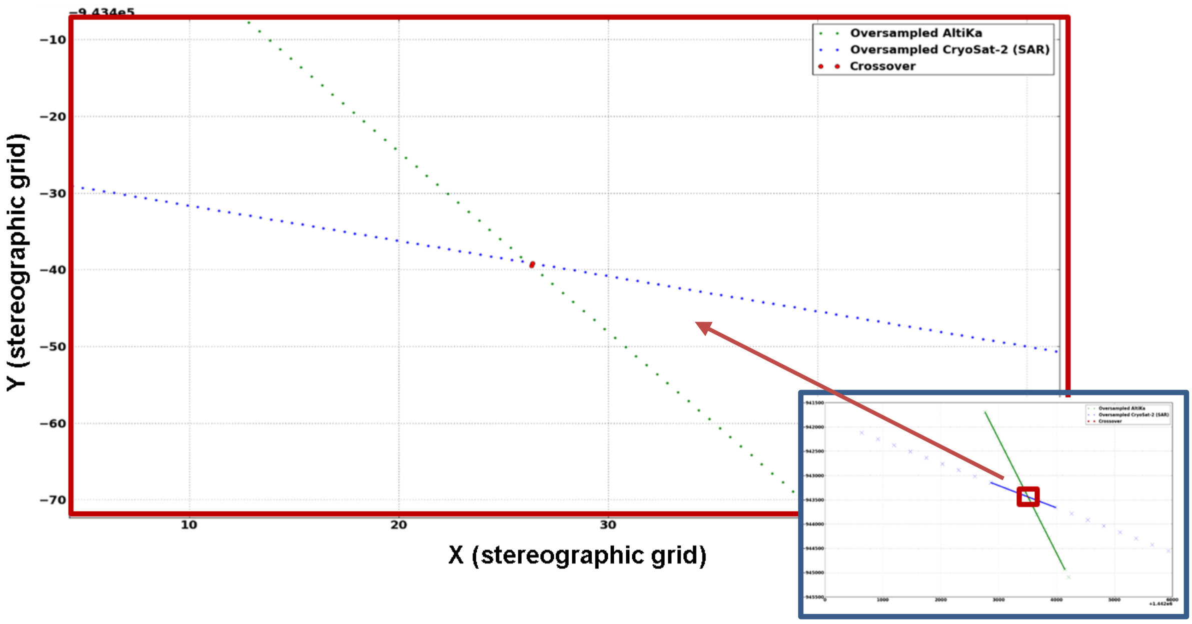


*Figure 32: Illustration of the method used to find the crossover point of the Cryosat-2 (blue) and AltiKa (green) tracks. Red box is a zoom of the bottom right figure, with circle dots representing the oversampled tracks*

The figure 33 shows the slight smoothing applied to the surface elevation estimated by AltiKa, along a track located around Vostok area:

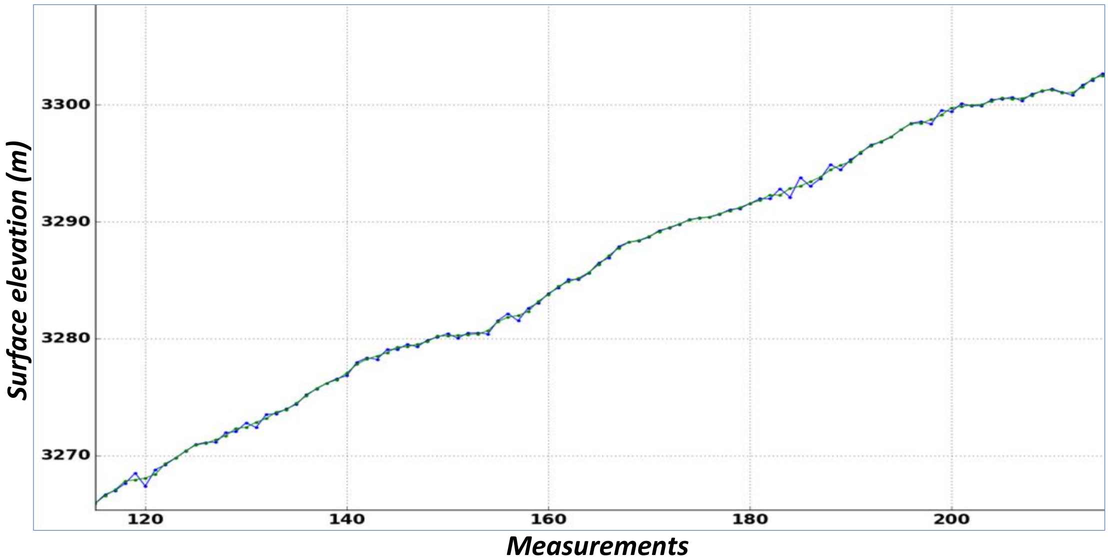


*Figure 33: Raw (blue) and smoothed (green) surface elevation estimated by AltiKa along a track located around lake Vostok*

## 6.3. Level 2 retrackers

At the end of SPICE phase 1, it has been decided to keep the following retrackers for Cryosat-2:

- SAR mode : **Threshold Peak Retracker (TPR)** retracker at **75%** threshold
- P-LRM : **Threshold Center Of Gravity (TCOG)** retracker at **50%** threshold

More details about these retrackers are available in RD-2 and RD-3. To estimate the altimeter range from AltiKa waveforms a TFMRA retracker has been choosen. As seen before, TPR and TFMRA have similar behaviours, these empirical retrackers output the first sample that reaches the amplitude set by a threshold. The only major difference for mono-peak waveforms is the waveform smoothing applied in TFMRA, before the maximum amplitude computation, to reduce speckle noise effects.

Over ocean, the LRM first surface return is estimated in the waveform leading edge at mid-power. Considering that AltiKa waveform leading edge remains visually steep on the ice-sheet analyzed waveforms (see section 5), a 50% threshold is set for retracking the AltiKa waveforms.

## 6.4. Results with the Cryosat-2 estimations from SPICE processing

### 6.4.1. AltiKa/Cryosat-2 crossovers

The following figures show the histograms of the surface elevation biases at crossovers, between AltiKa and Cryosat-2 in SAR mode (red) and P-LRM (green) over lake Vostok and DOME-C. As a reminder, respectively 42 and 50 crossovers have been analyzed over lake Vostok and Dome-C.

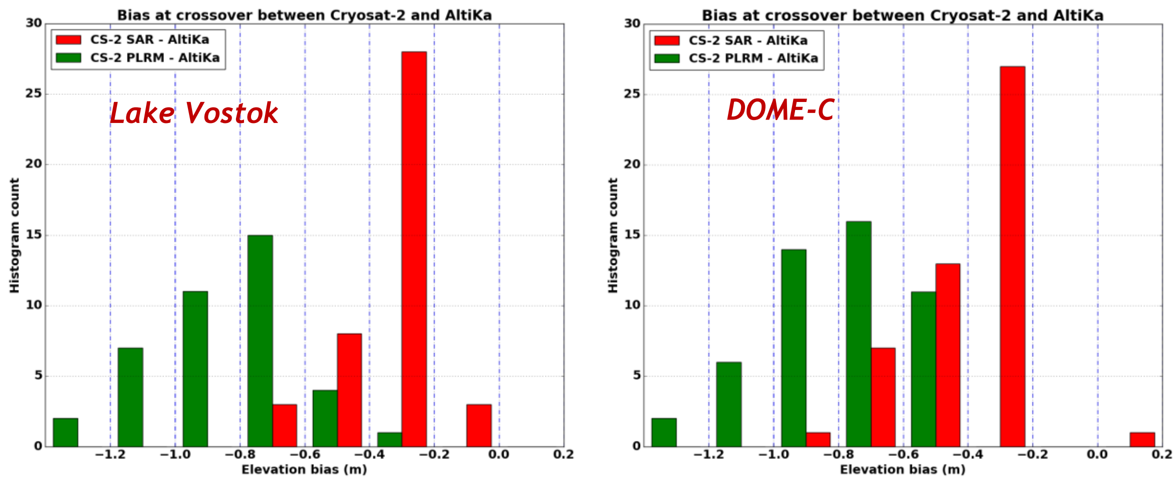


*Figure 34: Histograms of crossover biases between AltiKa and Croysat-2 over lake Vostok (left) and DOME-C (right)*

The following figures show the median surface elevation biases and standard deviation of AltiKa / Cryosat-2 crossovers, over lake Vostok and DOME-C.

| | | Lake Vostok | DOME-C |
|---|---|---|---|
| CS2 SAR - AltiKa | Median bias (m) | -0.34 | -0.38 |
| | STD (m) | 0.13 | 0.18 |
| CS2 P-LRM - AltiKa | Median bias (m) | -0.8 | -0.73 |
| | STD (m) | 0.25 | 0.2 |

*Table 2: Surface elevation biases and standard deviations at crossovers between Cryosat-2 and AltiKa over lake Vostok and DOME-C*

These results show that Cryosat-2 underestimates surface elevation by respectively 70 cm to 80 cm and 34 to 38 cm in P-LRM and SAR mode, compared to AltiKa. The AltiKa / Cryosat-2 measurement noise at crossover is reduced in SAR mode compared to PLRM, with a standard deviation between Cryosat-2 and AltiKa of respectively 13 cm and 18 cm in SAR mode, compared to 20 cm and 25 cm in P-LRM.

### 6.4.2. DEMs comparison over lake Vostok

To assess consistency with auxiliary data products, a comparison of altimetry to external DEMs over lake Vostok is now performed. Two DEMs are used:

- **1) Bamber DEM** [Bamber et al., 2009] computed from ERS-1 radar altimetry and ICESat laser altimetry. Time stamp: 2004. (more details regarding ICESat mission and its performances over ice sheet can be found in Brenner et al. [2007]).
- **2) Helm DEM** [Helm et al., 2014] computed from Cryosat-2 LRM/SARIn radar altimetry. Time stamp: 2012.

Even if Bamber DEM is dated 2004, comparisons with acquisitions from 2014 are possible because lake Vostok elevation has an equilibrated local ice-mass balance, meaning that surface elevation is very stable over time (see section 4.1). Both DEMs have a spatial resolution of 1 km. Surface elevation from DEMs is computed at the crossover point by bi-linear interpolation to be directly compared to altimetry estimations. The following figures show the histogram biases between altimetry data and DEMs over the 42 crossovers of lake Vostok:

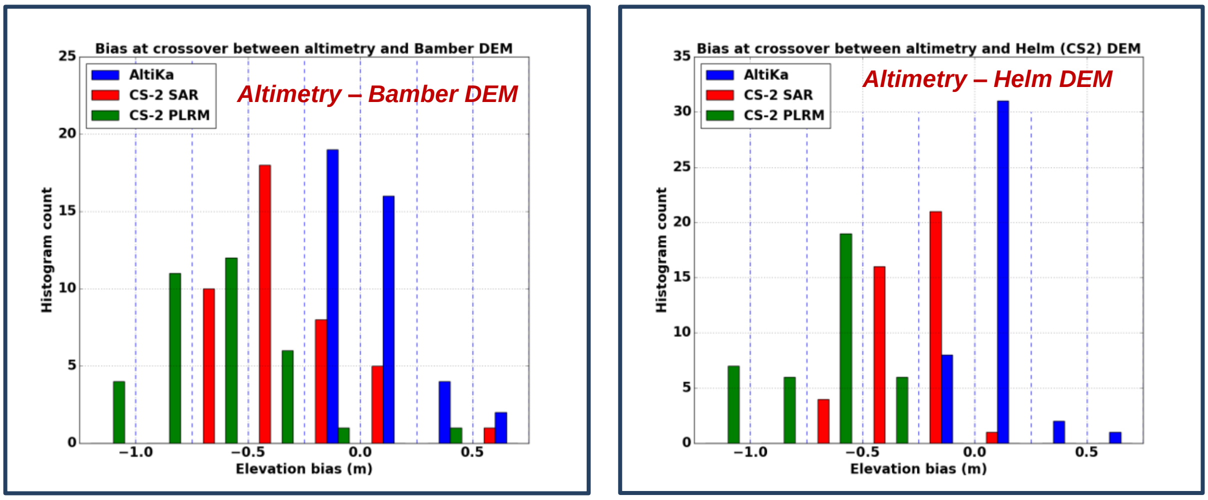


*Figure 35: Histogram of surface elevation biases between DEMs and three altimeter datasets: AltiKa (blue), Cryosat-2 in SAR mode (red) and Cryosat-2 in P-LRM (green)*

The following table presents the median biases and standard deviations between altimetry estimations and DEMs at 42 crossovers located over lake Vostok:

| | | Bamber DEM | Helm DEM |
|---|---|---|---|
| AltiKa LRM | Median bias (m) | +0.04 | +0.07 |
| | STD (m) | 0.24 | 0.12 |
| Cryosat-2 P-LRM | Median bias (m) | -0.79 | -0.68 |
| | STD (m) | 0.39 | 0.29 |
| Cryosat-2 SAR | Median bias (m) | -0.31 | -0.23 |
| | STD (m) | 0.26 | 0.15 |

***Table 3: Surface elevation biases and standard deviations between altimetry and DEMs at 42 AltiKa/Cryosat-2 crossovers located over the flat surface of lake Vostok***

<u>**Conclusions**</u>

Surface elevation from Cryosat-2 P-LRM and SAR mode is underestimated by respectively -70cm/-80cm and -20cm/-30cm compared to both DEMs. The SAR mode precision appears to be better than the P-LRM one: standard deviations with Helm and Bamber DEM are reduced by respectively 50% and 33%.

Regarding AltiKa, surface elevation is estimated at the same level than both DEMs. The Bamber DEM is generated with laser altimetry, and as the laser does not penetrate into the snowpack, it probably explained the good agreement with the Ka band measurements of AltiKa. On the other hand, Helm DEM is generated with Cryosat-2 conventional altimetry (LRM), sensitive to the volume scattering effect. But as [Helm et al., 2014] choose a low retracking threshold (25%), it certainly compensates the bias due to the volume scattering effect, as seen in section 5.4.

In conclusion, the underestimation of the surface elevation observed for Cryosat-2 is questionable:

- **Cryosat-2 PLRM:** As discussed in meetings, the 50% TCOG threshold used in P-LRM is equivalent to a TPR 35% threshold for ice sheet acquisitions. It is accountable for a part of the bias, but probably not the whole 70/80cm.

- **Cryosat-2 SAR:** The 75% threshold used for SAR Cryosat-2 waveforms corresponds to the first surface return over ocean, similarly to the LRM AltiKa 50% threshold. The leading edges of the ice-sheet waveforms appear as steep as the oceanic ones (section 5.3), at least until 80% of maximum power. Based on this result, we would have expected a better alignment of the LRM Ka and SAR Ku estimations.

To ensure that biases observed are due to geophysical phenomena and not retracker discrepancies, the SPICE Cryosat-2 L1B waveforms are now retracked with the same algorithm than used for AltiKa. Results are presented in the following section.

## 6.5. Results with the Cryosat-2 estimations from CLS TFMRA retracker

### 6.5.1. Methodology

The surface elevation is now estimated from Cryosat-2 measurements starting from the L1B waveforms delivered at the end of SPICE project phase 2, using the TFMRA retracker (see description section 6.3). The surface elevation is retrieved using the usual computation:

⇨ *Elevation = Satellite altitude - (range + epoch) – geophysical corrections*

Except for the epoch estimated with the TFMRA retracker, all the other variables come from SPICE L1B products. For the P-LRM waveforms, we choose the same threshold as [Helm et al., 2014] did for his publication: **25%.** With this threshold the range estimated is theoretically close to the snow/air interface (see section 5.4). Waveform analysis performed in section 5 shows that SAR mode leading edge remains steep over lake Vostok. Consequently, we choose a threshold of **80%** for SAR mode waveforms, corresponding approximately to surface first return over Ocean [Boy et al., 2017].

### 6.5.2. Croysat-2 / AltiKa crossovers

The following figures show histograms equivalent to those presented in section 6.4.1, providing surface elevation biases at crossovers, between AltiKa and Cryosat-2 in SAR mode (red) and P-LRM (green) over lake Vostok and DOME-C. As a reminder, respectively 42 and 50 crossovers have been analyzed over lake Vostok and Dome-C.

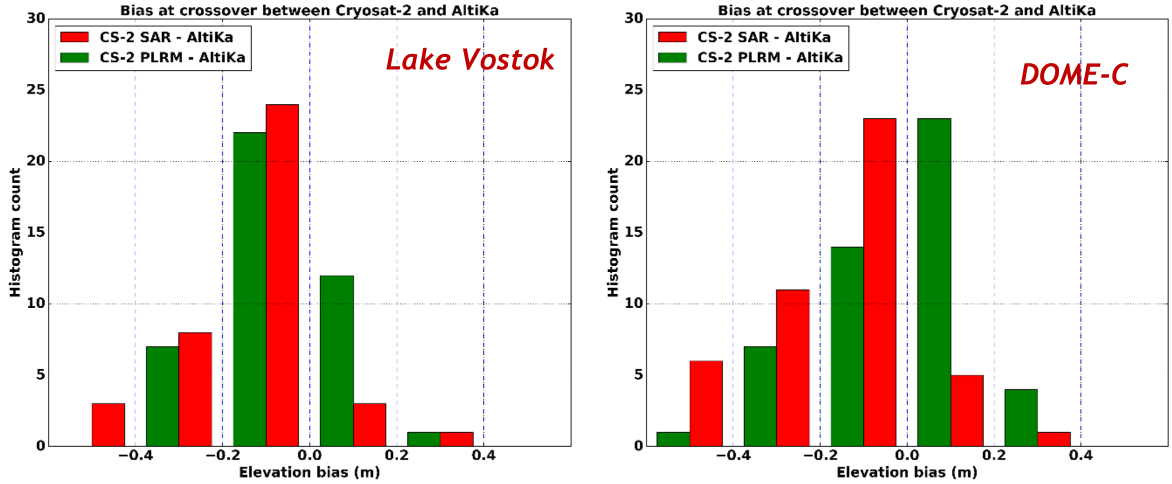


*Figure 36: Histograms of crossover biases between AltiKa and Croysat-2 over lake Vostok (left) and DOME-C (right) with CLS L2 processing*

The following figures show the median biases and standard deviations at crossovers, between AltiKa and Cryosat-2 over lake Vostok and DOME-C. In red color, with the updated results got from Cryosat-2 using TFMRA retracker.

| | | L2 from SPICE | | L2 from CLS | |
|---|---|---|---|---|---|
| | | Lake Vostok | DOME-C | Lake Vostok | DOME-C |
| CS2 SAR - AltiKa | Median bias (m) | -0.34 | -0.38 | -0.11 | -0.12 |
| | STD (m) | 0.13 | 0.18 | 0.21 | 0.24 |
| CS2 P-LRM - AltiKa | Median bias (m) | -0.8 | -0.73 | -0.06 | +0.004 |
| | STD (m) | 0.25 | 0.2 | 0.13 | 0.16 |

***Table 4: Surface elevation biases and standard deviations at crossovers between Cryosat-2 and AltiKa over lake Vostok and DOME-C. Left, with Cryosat-2 estimations from SPICE; right with Cryosat-2 estimations from CLS***

The offset between Cryosat-2 and AltiKa is now reduced with the Cryosat-2 elevations estimated from TFMRA algorithm. SAR mode of Cryosat-2 now underestimates surface elevation of around **10cm,** compared to 34/38cm from SPICE data**.** More significantly, P-LRM of Cryosat-2 and LRM of AltiKa are now almost perfectly in line.

As explained in the previous section, by setting the threshold of the TFMRA retracker at 50% for AltiKa and 80% for the SAR mode of Cryosat-2, the alignment of both missions is expected. The slight underestimation got from SPICE, using a similar retracker should be investigated. On the other hand, SAR Cryosat-2 estimations from SPICE are more precise, with a standard deviation reduced from 21cm to 13cm over lake Vostok compared to CLS TFMRA retracker.

For Cryosat-2 P-LRM we have deliberately lowered the TFMRA threshold at 25% of maximum power, following Davis recommendations [1997] and to be in accordance with Helm et al. [2014]. Over relative smooth surfaces as encountered in the continent’s interior, this threshold corresponds in average to the estimate of the ice-sheet elevation at snow/air interface. In our study, it provides a correct alignment with AltiKa over lake Vostok and Dome-C. The mean bias at crossovers is respectively only +6 cm and +0,4 cm for both areas.

The 70 / 80 cm underestimation got from P-LRM SPICE estimations should be investigated in a future study. As discussed in meeting, the 50% threshold of the TCOG retracker corresponds approximately to a 35% threshold for a TPR / TFMRA retracker. In our opinion, such a slight difference on the threshold values (35% vs 25%) should not create a so important difference on the surface elevation estimated.

### 6.5.3. Comparison with DEMs

The following figures show the histogram of the biases between altimetry data and DEMs over the 42 crossovers of lake Vostok using the Cryosat-2 estimations from CLS TFMRA retracker.

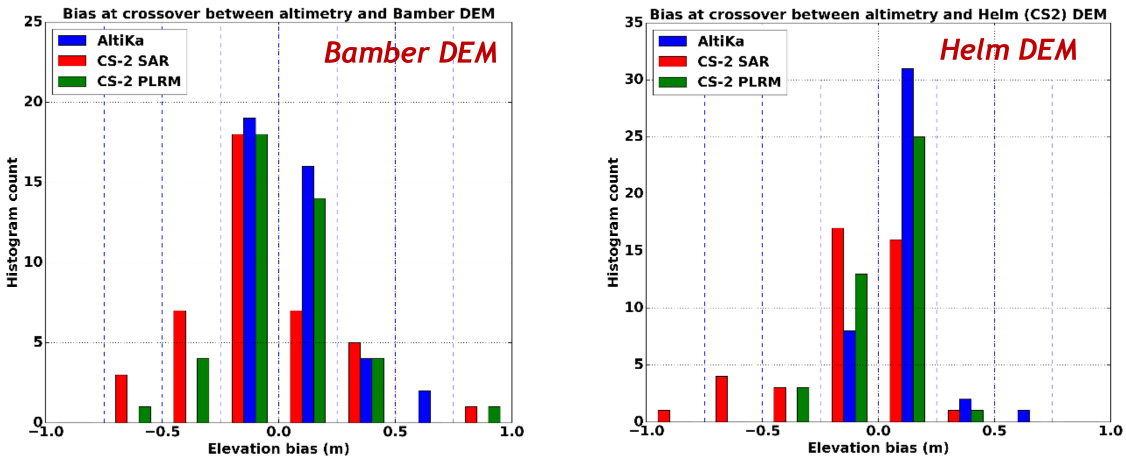


*Figure 37: Histogram of surface elevation biases between DEMs and three altimeter datasets: AltiKa (blue), Cryosat-2 in SAR mode (red) and Cryosat-2 in P-LRM (green)*

The following table presents the median biases and standard deviations between altimeter estimations and DEMs on 42 crossovers located over lake Vostok:

| | | Bamber DEM | Helm DEM |
|---|---|---|---|
| AltiKa LRM | Median bias (m) | +0.04 | +0.07 |
| | STD (m) | 0.24 | 0.12 |
| Cryosat-2 P-LRM | Median bias (m) | -0.02 | +0.03 |
| | STD (m) | 0.27 | 0.16 |
| Cryosat-2 SAR | Median bias (m) | -0.08 | -0.03 |
| | STD (m) | 0.33 | 0.24 |

*Table 5: Bias and standard deviation between altimetry and DEMs at the 42 AltiKa/Cryosat-2 crossovers located over the flat surface of lake Vostok*

This last result shows that the three modes are accordingly at the same level than the two DEMs studied. This was expected for Cryosat-2 P-LRM estimations considering that Helm build his DEM with LRM Cryosat-2 data equally retracked (TFMRA with same 25% threshold).

This demonstrates that, over the smooth surfaces of the Antarctica plateau, a LRM / P-LRM 25% threshold in Ku band, a LRM 50% threshold in Ka band, and a SAR 80% threshold in Ku band provides a good alignment of the three measures, with +/- 10cm of difference.

Standard deviation between altimetry and DEMs is much lower using Helm DEM compared to Bamber DEM. We do not have yet a clear explanation to this result. Probably the geodetic orbit of Cryosat-2 provides a better spatial coverage than Bamber had with ERS, leading to a better homogeneity of the DEM.

Finally, we examine the three measures precision: LRM Ku / LRM Ka / SAR Ku. Most probably due to its Ka band, less sensitive to volume scattering, AltiKa standard deviation is the lowest of the three measures. In contrast, because of its high retracking threshold (80%), the speckle noise has more influence on the SAR Ku estimations, explaining the worst precision of Cryosat-2 SAR estimations compared to the two others measures. P-LRM precision are in between, still slightly worse than AltiKa even with the lower threshold used (25% compared to 50% for AltiKa).

## 7. Surface anisotropy at crossovers

The objective of this study is to compare polarization effects in Ku and Ka band and analyze the surface anisotropy and its impact on SAR measurement. In fact, it is well known that the echo volume intensity as measured by the altimeter is modulated by the angle between the antenna polarization direction and the prevailing surface anisotropy direction. This effect appears only on sloppy surface with volume echo. It may be detected by analyzing the backscatter difference at cross-overs between ascending and descending tracks (see for example Remy et al. [2012].

The first part, comparison between Ku and Ka band, was already performed for LRM Ku and Ka band by comparing the polarization effects of Envisat and AltiKa [Rémy et al., 2015]. We show that the polarization effect on backscatter is larger for Ka band than Ku band. Indeed, the volume echo is larger for ka band and comes from the near sub-surface. In term of impact on height, the effect is smaller for Ka band because of the smaller penetration depth. For the impact on SAR measurements, we initially propose to analyse cross-overs differences of SAR data with other missions, such SARAL/AltiKa in order to detect both volume and surface anisotropy impact on SAR waveform.

However, since the writing of the project, studies performed at CLS have shown, thanks to a SAR echo simulator and the analyze of SAR Cryosat-2 acquisitions, that the SAR altimetry mode is not affected by the along-track slope [Aublanc et al., 2017]. Only across-track slope plays a role. This means that SAR waveform shapes are sensitive to the flight direction with respect to the surface slope. This adds an unknown in the across-slope analysis whose effect is probably dominant over anisotropic effects because of the low sensitivity to volume echo for SAR mode on leading edge of the waveform, and of the same order of magnitude on backscatter. The SAR backscatter difference at cross-over points is then controlled by the 2-D local surface slope and the local anisotropic effect, thus by 3 parameters. Note that the comparison between PLRM of Cryosat-2 and the LRM of AltiKa would probably give the same results as the comparison between LRM of Envisat and of AltiKa, already done.

Moreover, to study anisotropy we may choose the SPIRIT zone because the Vostok and the Dome-C area are too flat. Cryosat-2 ascending/descending crossovers studied in section 5.5 confirm there is no anisotropy effect on Vostok and DOME-C area. In the SPIRIT area, we have only 5 cross-overs for the SAR data that prevents to properly do statistics (see Figure 8). We have about 20 cross-overs differences between Cryosat-2 and SARAL data (see Figure 8) but the surface slope at these points is too high for Ka measurements whose half antenna aperture is 0.305° or 5.2 m/km. We have only two valid cross-over differences.

So we think that this study, due to this new underestimated equation, is infeasible because of the poor number of valid cross-overs in the SPIRIT zone.

## 8. Conclusions

This study was the opportunity to assess the radar signal interaction with the Antarctica snowpack in different altimetry modes (LRM / SAR) and bands (Ku / Ka). This has been made possible thanks to a first set of SAR altimetry measurements acquired over the Antarctica ice sheets by the Cryosat-2 spacecraft in winter 2014. Even if the number of Cryosat-2 and AltiKa crossovers are limited, **several robust conclusions can be drawn from this work:**

- **In P-LRM Ku band,** the Cryosat-2 waveforms have a typical shape already observed on other LRM missions (ERS & Envisat). The waveform leading edge is significantly distorted by the volume scattering effect, particularly from mid-power.
- **In SAR Ku band,** thanks to the specific surface sampling of the SAR altimetry measure, the waveform leading edge remains relatively peaky, and is therefore weakly sensitive to volume scattering. This would facilitate the estimation of a stable, repeatable, surface elevation.
- **In LRM Ka band,** as expected, the waveform is weakly impacted by volume scattering, demonstrating the Ka benefit over ice surfaces. Nevertheless, there is a non-negligible part of the measured energy coming from the snowpack interior, modifying slightly the waveform shape when compared to an oceanic measurement.
- An AltiKa / Cryosat-2 crossover analysis performed over the flat surface of lake Vostok shows that the surface elevation estimated on the three measures are aligned when epoch is positioned around:
  - 25% of maximum power in LRM / P-LRM Ku band
  - 80% of maximum power in SAR Ku band
  - 50% of maximum power in LRM Ka band
- These estimations are also consistent with two Antarctica DEMs (Bamber & Helm). By a GNSS analysis, Schröder et al. [2017] shows that both DEMs underestimate surface elevations from 20cm around. Hence, the altimetry estimations might still underestimate the snow/air interface of around 20 cm.
- This comparison is performed with austral spring acquisitions. Other studies show that seasonal variations of the snow properties modify the waveform shape in LRM Ku band [Lacroix et al., 2007 ; Lacroix et al., 2009]. This consequently impacts the surface elevation estimated by empirical retrackers. A similar study must be conducted with measurements acquired all along the year.

Finally, this study is one of the rare exploiting both potentials of the Ka and Ku bands at crossovers, unfortunately only over a limited space and time period. The recent launch of the Sentinel-3A mission in 2016 and its full SAR coverage opens new perspectives for a more complete study, over the whole Antarctica and Greenland ice sheets. This will help defining and designing the future Cryosat-3 mission, planned with a double Ku/Ka frequency band.

# List of Acronyms

| | |
|---|---|
| CLS | Collecte Localisation Satellite |
| CNES | Centre National d'Etude Spatiale |
| CPP | Cryosat-2 Processing Prototype |
| DEM | Digital Elevation Model |
| EPSG | European Petroleum Survey Group |
| ERS | ESA Remote Sensing |
| ESA | European Space Agency |
| GNSS | Global Navigation Satellite System |
| ISRO | Indian Space Research Organisation |
| LRM | Low Resolution Mode |
| MODIS | Moderate-Resolution Imaging Spectroradiometer |
| P-LRM | Pseudo Low Resolution Mode |
| PRF | Pulse Rate Frequency |
| PDGS | Payload Data Ground Segment |
| POCA | Point Of Closest Approach |
| RD | Reference Document |
| SAR | Synthetic Aperture Radar |
| SARM | Synthetic Aperture Radar Mode |
| SARIn | Synthetic Aperture Radar INterferometric |
| SARAL | Satellite with ARgos and ALtika |
| SPICE | Sentinel-3 Performance improvement for ICE sheets |
| SPIRIT | SPOT-5 stereoscopic survey of Polar Ice: Reference Images and Topographies |
| SIRAL | SAR Interferometric Radar ALtimeter |
| STD | STandard Deviation |
| TCOG | Threshold Center Of Gravity |
| TFMRA | Threshold First Maximum Retracking Algorithm |
| TPR | Threshold Peak Retracker |
| SWH | Significant Wave Height |

## References

Armitage, T., Wingham, D., Ridout, A., 2014, Meteorological Origin of the Static Crossover Pattern Present in Low-Resolution-Mode CryoSat-2 Data Over Central Antarctica, IEEE GEOSCIENCE AND REMOTE SENSING LETTERS, VOL. 11, NO. 7, JULY 2014

Aublanc, J., Moreau, T., Thibaut, P., Boy, F., Rémy, F., and Picot, N., 2018, Evaluation of SAR Altimetry over the Antarctic Ice Sheet from CryoSat-2 acquisitions , ASR (forthcoming), https://doi.org/10.1016/j.asr.2018.06.043

Bamber, J. L. 1994, Ice sheet altimeter processing scheme, Int. J. Remote Sens., 15, 925-938

Bamber, J. L., J. L. Gomez-Dans 2009, A New 1 km Digital Elevation Model of the Antarctic Derived from Combined Satellite Radar and Laser Data Part 1: Data and Methods, The Cryosphere, 3, 101-111

Bentley J.L, 1975, Multidimensional binary search trees used for associative searching. Commun. ACM, 18(9):509–517.ISSN 0001-0782.

Boy, F., J-D. Desjonquères, N. Picot, T. Moreau, and M. Raynal 2017, CRYOSAT-2 SAR Mode Over Oceans: Processing Methods, Global Assessment and Benefits, IEEE Trans. Geosci. Remote Sens., 55, 148-158

Brenner, A. C., DiMarzio, J. R., and Zwally, H. J., 2007, Precision and accuracy of satellite radar and laser altimeter data over the continental ice sheets, IEEE T. Geosci. Rem. Sens., 45, 321–331

Brooks, R.I., Campbell, W.J., Ramseier, R.O., Stanley, H.R., Zwally, H.J. 1978, Ice sheet topography by satellite altimetry. Nature 274, 539–543

Davis, C. 1997, A robust threshold retracking algorithm for measuring ice-sheet surface elevation change from satellite radar altimeters, IEEE Trans Geosci Remote Sens 35, 974-979

Ekaykin, A. A., V. Y. Lipenkov, I. N. Kuzmina, J. R. Petit, V. Masson-Delmotte, and S. J. Johnsen, 2004, The changes in isotope composition and accumulation of snow at Vostok station, East Antarctica, over the past 200 years, Ann. Glaciol.,39, 569–575.

Ewert, H., Popov S.V., Richter, A., Schwabe, J., Scheinert, M., Dietrich, R., 2012, Precise analysis of ICESat altimetry data and assessment of the hydrostatic equilibrium for subglacial Lake Vostok, East Antarctica, Geophysical Journal International, Volume 191, Issue 2, Pages 557–568

Femenias, P., Remy, F., Raizonville, R., Minster, J.F. 1993, Analysis of satellite-altimeter height measurements above continental ice sheets. J. Glaciol., 39, 591-600

Helm, V., Humbert, A., & Miller, H. 2014, Elevation and elevation change of Greenland and Antarctica derived from CryoSat-2, The Cryosphere, 8(4), 1539-1559

Lacroix, P., M. Dechambre, B. Legresy, F. Blarel and F. Remy 2007, On the use of the dual-frequency ENVISAT altimeter to determine snowpack properties of the Antarctic ice sheet, Remote Sens. Environ., 112 (4), 1712–1729

Lacroix, P., Legresy, B., Remy, F., Blarel, F., Picard, G., Brucker, L., 2009, Rapid change of snow surface properties at Vostok, East Antarctica, revealed by altimetry and radiometry. Remote Sensing of Environment, 113 (12), 2633–2641.

Legresy, B.; Remy, F., 1998, Using the temporal variability of satellite radar altimetric observations to map surface properties of the Antarctic ice sheet. J. Glaciol., 44, 197-206.

Legrésy, B., Rémy, F., Schaeffer, P.,1999 ; Different ERS altimeter measurements between ascending and descending tracks caused by wind induced features over ice sheets, Geophysical Research letters, vol.26, issue 15, 2223-2407

Michel, A., Flament, T., Rémy, F., 2014, Study of the Penetration Bias of ENVISAT Altimeter Observations over Antarctica in Comparison to ICESat Observations, Remote Sensing, 6(10), 9412-9434;

Palerme et al., 2017, Evaluation of Antarctic snowfall in global meteorological reanalyses

Prandi, P.; Philipps, S.; Pignot, V.; Picot, N., 2015, SARAL/AltiKa global statistical assessment and cross-calibration with Jason-2. Mar. Geod., 38, 297–312, doi:10.1080/01490419.2014.995840.

Prandi, P.; Debout, V., 2016, SARAL/Altika validation and cross calibration activities, AVISO annual report, https://www.aviso.altimetry.fr/fileadmin/documents/calval/validation_report/AL/annual_report_al_2016.pdf

Raney, R.K. 1998, The delay/Doppler radar altimeter, IEEE Trans. Geosci. Remote Sens., 36, 1578–1588

F. Rémy, B. Legrésy, and J. Benveniste, 2006, “On the azimuthally anisotropy effects of polarisation for altimetric measurements,” IEEE Trans. Geosci. Remote Sens., vol. 44, no. 11, pp. 3289–3296,

Remy, F. and Parouty, S. 2009, Antarctic ice sheet and radar altimetry: A Review, Remote Sensing 1, 1212–1239

Remy, F., T. Flament, F. Blarel, and J. Benveniste 2012, Radar altimetry measurements over Antarctic ice sheet: A focus on antenna polarization and change in backscatter problems, Adv. Space Res. 2012, 50, 998–1006

Remy, F., Flament, T., Michel, A., Blumstein, D., 2015, Envisat and SARAL/AltiKa Observations of the Antarctic Ice Sheet: A Comparison Between the Ku-band and Ka-band, Marine Geodesy, 38:sup1, 510-521, DOI: 10.1080/01490419.2014.985347

Richter, A., et al. 2014, Height changes over subglacial Lake Vostok, East Antarctica: Insights from GNSS observations, J. Geophys. Res. Earth Surf., 119, 2460–2480, doi:10.1002/2014JF003228

Ridley, J. K. and K. C. Partington 1988, A model of satellite radar altimeter return from ice sheets, Int. J. Remote Sens., 9(4), 601–624

Rott, H.; Sturm, K.; Miller, H., 1993, Active and passive microwave signatures of Antarctic firn by means of field measurements and satellite data. Ann. Glaciol., 17, 337-343.

Sandwell, D. and Smith, W. 2014, Slope correction for ocean radar altimetry, Journal of Geodesy

Schröder et al., 2017, Validation of satellite altimetry by kinematic GNSS in central East Antarctica, The Cryosphere, 11, 1111-1130

Siegert, MJ., 2005, Lakes beneath the ice sheet: The occurrence, analysis and future exploration of Lake Vostok and other Antarctic subglacial lakes. Annual Reviews of Earth and Planetary Sciences, Vol. 33, 2005, p. 215 – 245

Steunou, N., Desjonquères, J. D., Picot, N., Sengenes, P., Noubel, J. & Poisson, J. C., 2015 AltiKa Altimeter: Instrument Description and In Flight Performance, Marine Geodesy, 38:sup1, 22-42, DOI: 10.1080/01490419.2014.988835.

Vincent, P., N. Steunou, E. Caubet, L. Phalippou, L. Rey, E. Thouvenot, and J. Verron. 2006. AltiKa: A Ka-band altime-try payload and system for operational altimetry during the GMES period. Sensors 6:208–234Wingham, D.J., Rapley, C.G., Griffiths, H., 1986. New techniques in satellite tracking system. Proceedings of IGARSS' 88 symposium, Zurich, pp. 1339–1344.

Wingham, D. J., Phalippou, L., Mavrocordatos C., and D. Wallis 2004, The mean echo and echo cross product from a beamforming interferometric altimeter and their application to elevation measurement, IEEE Trans. Geoscience and Remote Sensing, v. 42, No. 10